A Szilikátipari Tudományos Egyesület lapja

# építőanyag

Journal of Silicate Based and Composite Materials

## A TARTALOMBÓL:



2025/1

**Fórizs Katalin**
***(1959-2025)***

Fórizs Katalin 1959-ben született Egercsehiben. Az egri Gárdonyi Géza Gimnázium kémia-biológia tagozatán érettségizett. Ezt követően a Bélapátfalvi Cementgyár laboratóriumában kezdett dolgozni. Munkája mellett végezte vegyészmérnöki tanulmányait, 1986-ban kapta meg oklevelét a Veszprémi Vegyipari Egyetem Szilikátkémiai és Technológiai ágazatán.

Laboratóriumvezetői feladatai mellett érdeklődése egyre inkább a röntgenspektrometriás vizsgálatokra irányult. A Bélapátfalvi Cementgyár bezárása után 2002-től a Holcim Hungária Zrt. Miskolci (Hejőcsabai), majd később a Lábatlani Cementgyárában volt laborvezető. Ekkora már a hazai cementipar elismert röntgenanalitikai szakértője lett.

A Holcim Hungária Zrt. cementgyárainak bezárása után a SZIKKTI Labor Szilikátkémiai Anyagvizsgáló-Kutató Kft. laborvezetője lett, ahol főleg az üveg-, finom-és durvakerámia-, tűzállóanyag-, cement- és mészipari cégek részére végzett vizsgálatokat. Hosszú időn át vállalt szakértői feladatokat a vizsgálati szabványok hazai kiadásában. Mindig maximalista volt, munkáját alaposság jellemezte.

Kedves személyisége, vidám természete, óriási szakmai tudása meghatározó a SZIKKTI Labor mindennapjaiban. A hazai szilikátipar egy rendkívül precíz, hatalmas ismerettel és több évtizedes tapasztalattal rendelkező szakembert vesztett el; a röntgenspektrometria területén bizonyosan a legjobbat. Emberileg és szakmailag is pótolhatatlan.

Drága Kati! Sokat tanultunk Tőled, nem csak a szakmáról, a szakma szeretetéről, hanem az élet számos területéről. Biztosak vagyunk abban, hogy fentről továbbra is figyelsz ránk. Amilyen csendesen éltél, olyan csendben hagytál itt minket. Csendes legyen álmod, találj odafönt örök boldogságot! Emlékedet örökké őrizzük.

SZIKKTI Labor Szilikátkémiai

Anyagvizsgáló-Kutató Kft.

építőanyag
Journal of Silicate Based and Composite Materials
2025/1

## TARTALOM



## CONTENT



**A finomkerámia-, üveg-, cement-, mész-, beton-, tégla- és cserép-, kő- és kavics-, tűzállóanyag-, szigetelőanyag-iparágak szakmai lapja**
**Scientific journal of ceramics, glass, cement, concrete, clay products, stone and gravel, insulating and fireproof materials and composites**



A folyóiratot referálja · The journal is referred by:
A folyóiratban lektorált cikkek jelennek meg.
All published papers are peer-reviewed.
Kiadó · Publisher: Szilikátipari Tudományos Egyesület (SZTE)
Elnök · President: ASZTALOS István
1034 Budapest, Bécsi út 120.
Tel.: +36-1/201-9360 ▪ E-mail: epitoanyag@szte.org.hu
Tördelő szerkesztő · Layout editor: NÉMETH Hajnalka
Címlapfotó · Cover photo: BIRÓ András



WWW.EPITOANYAG.ORG.HU
EN.EPITOANYAG.ORG.HU

Online ISSN: 2064-4477
Print ISSN: 0013-970x
INDEX: 2 52 50 ▪ 77 (2025) 1-28

# Characterization of hair-sisal-glass fibre polyester hybrid composite materials

**Fikadu BELAY** ▪ Worabe University, Ethiopia ▪ fikadubelay249@gmail.com
**Abreham DEBEBE** ▪ Addis Ababa Science and Technology University, Ethiopia ▪ debebeabreham@yahoo.com
Érkezett: 2024. 04. 25. ▪ Received: 25. 04. 2024. ▪ https://doi.org/10.14382/epitoanyag-jsbcm.2025.1

**Abstract**
This study investigates the mechanical properties of Hair/Sisal/Glass Fiber Reinforced Polyester plastic (HSGFRP) hybrid composites composed of 15% fiber content by weight, with equal proportions of hair, sisal, and glass fibers, and 85% polyester matrix. However, to ensure accuracy in representing the material composition, the fiber content was recalculated and expressed in terms of volume fraction (vol%), considering the differences in densities among the fibers and the matrix material. Based on this adjustment, the total fiber content corresponds to approximately 7.67% by volume, with equal volumetric proportions of hair, sisal, and glass fibers. Specimens fabricated using the hand lay-up technique were tested for tensile, flexural, impact, and water absorption properties. The HSGFRP achieved 53% of the tensile strength, 94% of the flexural strength, and 77% of the impact strength of Glass Fiber Reinforced Composite (GFRP), with moderate water absorption properties comparable to glass and glass/sisal fiber materials. The addition of glass fiber enhanced tensile and flexural strength while reducing impact strength. HSGFRP exhibits balanced mechanical properties, making it a viable, lightweight, and cost-effective alternative to traditional glass fiber composites for light-load applications, despite a noticeable gap in tensile strength compared to GFRP.
Keywords: hair fibre, hair/sisal fibre, hair/sisal/glass fibre, polyester hybrid plastics
Kulcsszavak: hajszál, haj/szizál szál, haj/szizál/üvegszál, poliészter hybrid műanyagok

**Fikadu BELAY**
graduated with a Bachelor of Science degree in Mechanical Engineering from Wollo University and earned his Master's degree in Mechanical Engineering Design from Addis Ababa Science and Technology University. He is currently working as a lecturer at Menschen für Menschen Agro-Technical and Technology College. He has also taught at Mizan-Tepi University and Werabe University. His areas of interest include mechanical design, mechatronics, simulation-based engineering, and renewable energy systems. He is passionate about applying engineering solutions to address practical challenges in his community.

**Abraham Debebe WOLDEYOHANNES**
(PhD) is currently working as an Associate professor in Mechanical Engineering. Prior to joining the current position, Woldeyohannes was working as Director General at the Ministry of Innovations and Technology for one year. Woldeyohannes has more than 23 years of experience in higher education accumulating teaching and learning, research and leadership working in Ethiopia, Malaysia and Oman in different positions before holding the current position. His research interest focuses on applied operations research, Advanced Manufacturing system, manufacturing system optimization, and Modelling and performance analysis of flexible manufacturing / assembly systems and composite materials.

## 1. Introduction

The hybridization of natural and synthetic fibers has gained significant attention in recent years due to its potential to enhance the mechanical properties of composite materials while reducing both costs and environmental impact. Chemical treatments, such as alkaline and acrylic acid treatments, have been shown to further improve the mechanical properties of natural fiber-reinforced plastics, including tensile, flexural, and impact strength, as well as water resistance [1, 2].

Various composite materials have emerged by combining natural, synthetic, and hybrid fibres. Glass fibre, a widely used synthetic option, is known for its excellent mechanical properties, including tensile strength, stiffness, and impact resistance, making it versatile for engineering applications. Hybridizing glass fibre with natural fibres like sisal enhances the strength, particularly in impact resistance. However, factors such as impurities and volume percentage of reinforcements can affect mechanical properties [3-6].

Hair fibre, an underutilized natural option, shows promise in reinforcing composites, improving properties like compressive and bending strength, as well as water uptake. It has been explored for specific applications like engine piston materials, displaying notable resistance to creep, stiffness, and temperature [7-9].

Similarly, sisal fibre has been extensively used as a reinforcement, with studies focusing on fibre treatment effects on tensile strength, flexural strength, and water resistance. Evaluations at different fibre loadings reveal varied impacts on ductility, stiffness, and hardness [10-14].

This study aims to compare the mechanical properties of hair, sisal, and glass fibre-reinforced plastics, along with hybrid combinations. By analyzing the mechanical behaviors of these materials, the goal is to identify the most effective reinforcement combinations to improve their performance in engineering applications.

## 2. Materials and methods

### 2.1 Materials used

**Hair fibre:** Is collected from a local barber shop. It is washed with water and sun dried to free it from its oil and dusts content before treatment. Next it is soaked with 5% alkaline (NaOH) for twenty-four hours to improve their hydrophilic nature and sun dried again. Lastly, short fibres weighted based on their percentage and distributed evenly to form a lamina of hair fibre.

**Sisal fibre:** Is extracted from the sisal plant from local farm manually. Sisal fibre is then washed with water and sun dried to free it from its oil and dusts content. And it is soaked with 5% alkaline (NaOH) for twenty-four hours to improve their hydrophilic nature and sun dried again. At the end dried sisal fibre is chopped and layer is formed with randomly distributing the short fibres.

**Glass fibre:** is bought from the local market of water proof work Addis Ababa Ethiopia. Then weighted and in the form of layer to fit the Mold size.

**Polyester resin:** The type of polymer used in the recent research is a general-purpose unsaturated polyester known as TOPAZ-1110 TP which is collected from local fiberglass water proof manufacturing.

| Fibers | Tensile modulus (E) (GPa) | Tensile strength (σ) (MPa) | Density (ρ) (g/cm³) |
|---|---|---|---|
| **E – glass** | 69 | 2400 | 2.54 |
| **Hair** | 1.74 – 4.39 | 380 - 400 | 1.32 |
| **Sisal** | 9.4 – 22 | 400 - 700 | 1.45 |
| **Resin (Polyester)** | 2.0 – 4.5 | 40 - 90 | 1.3 |

*Table 1 Mechanical properties of the constituent materials*
*1. táblázat Összetevők mechanikai tulajdonságai*

**Hardener (Methyl-Ethyl-Ketone-Peroxide) (MEKP):** The Hardener is the second part of the matrix which is mixed with polyester resin to facilitate the curing of the resulted composite materials.


*a) Sisal fiber*


*b) Hair fiber*


*c) Glass fiber*


*d) Resin and hardener*

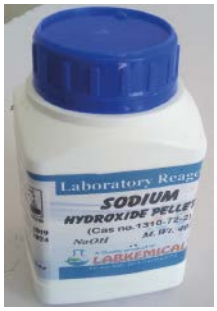

*e) NaOH*


*f) Distilled water*

*Fig.1 Materials used for composite preparation*
*1. ábra Kompozit készítéshez alkalmazott anyagok*

## 2.2 Preferred fibre to matrix weight percentage

The composite materials were prepared with a fiber-to-matrix ratio of 15% and 85% by weight, respectively, based on the observation that the sisal-hair fiber reinforced composite exhibits maximum tensile, flexural, and impact strengths at this ratio. This weight percentage was initially chosen for consistency across all cases. However, expressing fiber content solely in terms of weight percentage is less accurate due to differences in densities between the fibers and the matrix material. To ensure scientific accuracy, the fiber content was recalculated and expressed in terms of volume fraction (vol%), where a 15% fiber content by weight corresponds to a total fiber volume fraction of approximately 7.67% [15]. This fixed fiber volume fraction was maintained across all configurations while varying the types of fibers to enable meaningful comparisons of mechanical properties. Eight distinct fiber-reinforced composite configurations were developed, including fully glass fiber, fully sisal fiber, fully hair fiber, glass and hair fibers, glass and sisal fibers, hair and sisal fibers, and a hybrid composite consisting of glass, hair, and sisal fibers. This adjustment ensures a more precise comparative investigation of mechanical properties while maintaining a constant total fiber volume fraction of 7.67% across all cases.

## 2.3 Volume, mass fraction and density of the samples

This research incorporates three types of fibres - hair, sisal, and glass fibre individually and in hybrid combinations, within a polyester thermosetting polymer matrix. Seven distinct composite types are developed by combining these fibres: glass fibre reinforced plastics (GFRP), sisal fibre reinforced plastics (SFRP), hair fibre reinforced plastics (HFRP), hair/sisal fibre reinforced plastics (HSFRP), hair/glass fibre reinforced plastics (HGFRP), sisal/glass reinforced plastics (SGFRP), and hair/sisal/glass fibre reinforced plastics (HSGFRP). Each composite type undergoes the preparation of five trial samples per tests and each result is recorded.
Where:

| | |
|---|---|
| $\boldsymbol{v}_{C,f,m}$ | Volume of composite, fiber and matrix respectively |
| $\boldsymbol{\rho}_{c,f,m}$ | Density of composite, fiber and matrix respectively |
| $\boldsymbol{m}_{c,f,m}$ | Mass of composite, fiber and matrix respectively |
| $\boldsymbol{\rho}_{f1,2,3\ldots n}$ | Density of the first, the second, the third and the nth fiber respectively |
| $\mathbf{m}_{\boldsymbol{f1,2,3\ldots n}}$ | Weight fraction of the first, the second and the nth fiber respectively |
| $\mathbf{W}_m, \boldsymbol{\rho}_m$ | Weight fraction and density of the matrix respectively |
| $\mathbf{W}_f, \boldsymbol{\rho}_f$ | Weight fraction and density of the fiber respectively |

The fiber Volume fraction ($V_f$) and the matrix volume fraction ($V_m$) can be calculated,

$$\mathbf{V}_f = \frac{\boldsymbol{v}_f}{\boldsymbol{v}_C} \text{ and } \mathbf{V}_m = \frac{\boldsymbol{v}_m}{\boldsymbol{v}_c} \quad (1)$$

Volume fraction of fiber and matrix can also be related as,

$$\mathbf{V}_f + \mathbf{V}_m = 1 \text{ and } \boldsymbol{v}_f + \boldsymbol{v}_m = \boldsymbol{v}_c \quad (2)$$

Weight fraction of fiber ($W_f$) and the matrix ($W_m$) are formulated as below,

$$\mathbf{W}_f = \frac{\boldsymbol{m}_f}{\boldsymbol{m}_C} \text{ and } \mathbf{W}_m = \frac{\boldsymbol{m}_m}{\boldsymbol{m}_c} \quad (3)$$

And similarly, the weight fraction of fiber and matrix can be related by,

$$\mathbf{W}_f + \mathbf{W}_m = 1 \text{ and } \boldsymbol{m}_f + \boldsymbol{m}_m = \boldsymbol{m}_c \quad (4)$$

From density of a material weight or mass of the corresponding material is given by,

$$\boldsymbol{m}_c = \boldsymbol{\rho}_c * \boldsymbol{v}_c, \boldsymbol{m}_f = \boldsymbol{\rho}_f * \boldsymbol{v}_f \text{ and } \boldsymbol{m}_m = \boldsymbol{\rho}_m * \boldsymbol{v}_m \quad (5)$$

Substitution of *Eq. (4)* back in to *Eq. (3)* it will give,

$$W_f = \frac{m_f}{m_c} = \frac{\rho_f * v_f}{\rho_c * v_c} = \frac{\rho_f}{\rho_c} * \frac{v_f}{v_c} = \frac{\rho_f}{\rho_c} V_f$$
$$W_m = \frac{m_m}{m_m} = \frac{\rho_m * v_m}{\rho_c * v_c} = \frac{\rho_m}{\rho_c} * \frac{v_m}{v_c} = \frac{\rho_m}{\rho_c} V_m \quad (6)$$

Again, the sum of weight of the fibers and the matrix will give us mass of the composite,

$$W_f + W_m = W_c \quad (7)$$

Adding $W_f$, $W_m$ and $W_c$ from *Eq. (3)* forward in to *Eq. (7)* give us,

$$\frac{1}{\rho_c} = \frac{W_f}{\rho_f} + \frac{W_m}{\rho_m} \quad (8)$$

For hybrid fiber reinforced composite, the above equations can be summarized to relate density, weight fraction of fibers and density of fibers as below. And all samples are prepared using this equation as a general formula.

$$\frac{1}{\rho_c} = \frac{W_{f1}}{\rho_{f1}} + \frac{W_{f2}}{\rho_{f2}} + \cdots \frac{W_{fn}}{\rho_{fn}} + \frac{W_m}{\rho_m} \quad (9)$$

| Types of samples | Types of fibre/s | Fibre percentage by weight (%) | Mass of fibre (g) | Mass of resin (polyester) with allowance (g) | Mass of hardener (g) |
|---|---|---|---|---|---|
| **GFRP** | Glass | 15 | 12.66 | 76.26 | 2 |
| **HFRP** | Hair | 15 | 11.88 | 72.97 | 2 |
| **SFRP** | Sisal | 15 | 12 | 73.73 | 2 |
| **HSFRP** | Hair | 7.5 | 5.97 | 72.34 | 2 |
| | Sisal | 7.5 | 5.97 | | |
| **HGFRP** | Hair | 7.5 | 6.16 | 74.4 | 2 |
| | Glass | 7.5 | 6.16 | | |
| **SGFRP** | Sisal | 7.5 | 5.24 | 74.4 | 2 |
| | Glass | 7.5 | 5.24 | | |
| **HSGFRP** | Hair | 5 | 4 | 73.6 | 2 |
| | Sisal | 5 | 4 | | |
| | Glass | 5 | 4 | | |

*Table 2. Mass percentage contribution of fibre and matrix*
*2. táblázat Ágyazóanyag és szál tömegszázalékos aránya*

## 2.4 Sample preparation

This research used hand lay-up method for sample preparation due to its simplicity, flexibility, and cost-effectiveness, especially when dealing with low-volume production or custom-made parts. The **hand lay-up method** involves manually placing layers of reinforcement fibers (such as glass, carbon, or natural fibers) in a mold, followed by the application of a resin system. This method allows for precise control of fiber placement and orientation, which is critical in achieving the desired mechanical properties of the composite part. Due to its adaptability, this method can accommodate a variety of **fiber orientations**, such as **unidirectional, bidirectional, or random orientations**, making it suitable for both simple and complex geometries.

One of the major advantages of the hand lay-up method is its ability to produce **customized composite parts** without the need for expensive machinery or molds. It is ideal for **prototype production, small-batch manufacturing**, and applications that require **structural reinforcement in specific directions**.


*a)*

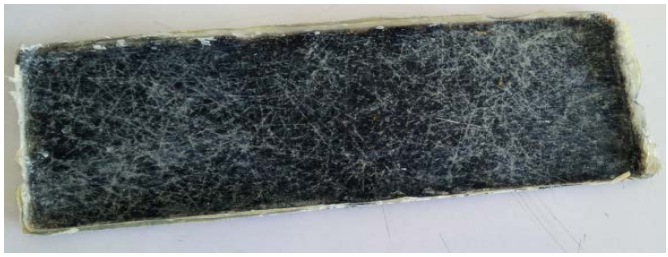

*b)*

*Fig. 2 a) Sample of Hair/glass fiber reinforced Plastics (HGFRP) for Flexural Test*
*b) Hair/glass fiber reinforced Plastics (HGFRP)*
*2. ábra a) Haj/üvegszál-erősítésű műanyag (HGFRP) minta hajlítószilárdság vizsgálathoz*
*b) Haj/üvegszál-erősítésű műanyag (HGFRP)*

## 2.5 Experiments conducted

### Tensile strength

Tensile test is done according to ASTM D638-03 with geometrical dimensions of 165 mm × 20 mm × 3 mm using UTM at the speed of 2mm/min [16, 17].

### Flexural strength

The three-point bending test sample is prepared based on ASTM D790 and its dimension is 125 mm × 13 mm × 3 mm with the speed of  using UTM [17].

### Impact strength

The sample for impact test is made using ASTM D256 with a dimension of 64 mm × 13 mm × 3 mm. Charpy impact testing is done on five samples for each case to measure the energy absorption capacity of the given materials. Impact energy is the difference in potential energies of the striking pendulum at the beginning position before a strike and at the end position after the strike of the sample [18].

### Water absorption test

Moisture absorption is done within distilled water using a very accurate techno test electronic balance and the sample is prepared according to ASTM D 570 which measures 30 mm × 28 mm × 3 mm [1].

## 3. Results and discussions

This section presents and analyzes the experimental results from the characterization of hair-sisal-glass fiber polyester

hybrid composites. Key material properties, including tensile strength, flexural strength, impact resistance, and water absorption, are examined in detail. The effects of fiber composition, fiber-matrix bonding, and hybridization on the overall mechanical performance of the composite are evaluated based on the experimental data. All mechanical test results are systematically presented for clarity and comparison in *Table 3.*

*a)*


*b)*


*c)*

*Fig. 3 a) Universal Testing Machine*
*b) Charpy impact Testing Machine*
*c) Electronic balance for Water Absorption Test*
*3. ábra a) Univerzális vizsgáló berendezés*
*b) Charpy kalapács*
*c) Elektromos mérleg vízfelvétel vizsgálathoz*

| Types of samples | | Tensile strength (MPa) | Flexural load (N) | Flexural strength (MPa) | Impact energy (J) |
|---|---|---|---|---|---|
| **GFRP** | GFRP1 | 43.3 | 90 | 144.23 | 11 |
| | GFRP2 | 41.28 | 50 | 80.13 | 11 |
| | GFRP3 | 55.13 | 70 | 112.18 | 12 |
| | GFRP4 | 40.51 | 90 | 144.23 | 9.5 |
| | GFRP5 | 36.41 | 50 | 80.13 | 7.5 |
| | *Average* | *43.33* | *70* | *112.18* | *10.2* |
| **HFRP** | HFRP1 | 16.28 | 20 | 112.18 | 10 |
| | HFRP2 | 18.97 | 20 | 32.05 | 6 |
| | HFRP3 | 17.69 | 20 | 32.05 | 7 |
| | HFRP4 | 10.26 | 20 | 32.05 | 5 |
| | HFRP5 | 18.21 | 20 | 48.08 | 9.5 |
| | *Average* | *16.28* | *20* | *51.28* | *7.5* |
| **SFRP** | SFRP1 | 20 | 20 | 32.05 | 4.5 |
| | SFRP2 | 16.15 | 50 | 80.13 | 7 |
| | SFRP3 | 17.44 | 20 | 32.05 | 6.5 |
| | SFRP4 | 16.41 | 40 | 64.1 | 5.5 |
| | SFRP5 | 23.85 | 40 | 64.1 | 7 |
| | *Average* | *18.77* | *34* | *54.49* | *6.1* |
| **HSFRP** | HSFRP1 | 22.8 | 40 | 64.1 | 6 |
| | HSFRP2 | 18.72 | 20 | 32.05 | 8.5 |
| | HSFRP3 | 30.26 | 20 | 32.05 | 11.5 |
| | HSFRP4 | 19.74 | 20 | 32.05 | 4.5 |
| | HSFRP5 | 22.56 | 40 | 64.1 | 8.5 |
| | *Average* | *22.82* | *28* | *44.87* | *7.8* |
| **HGFRP** | HGFRP1 | 28.97 | 50 | 80.13 | 5 |
| | HGFRP2 | 21.03 | 40 | 64.1 | 5 |
| | HGFRP3 | 18.46 | 50 | 80.13 | 7.5 |
| | HGFRP4 | 24.87 | 50 | 80.13 | 7.5 |
| | HGFRP5 | 18.72 | 50 | 80.13 | 11.5 |
| | *Average* | *22.41* | *48* | *76.92* | *7.3* |
| **SGFRP** | SGFRP1 | 19.87 | 70 | 112.18 | 4 |
| | SGFRP2 | 24.87 | 90 | 144.23 | 5 |
| | SGFRP3 | 15.64 | 70 | 112.18 | 5.5 |
| | SGFRP4 | 16.15 | 50 | 80.13 | 5.5 |
| | SGFRP5 | 22.82 | 50 | 80.13 | 8.5 |
| | *Average* | *19.87* | *66* | *105.77* | *5.7* |
| **HSGFRP** | HSGFRP1 | 22.37 | 70 | 112.18 | 7.5 |
| | HSGFRP2 | 29.74 | 50 | 80.13 | 10 |
| | HSGFRP3 | 19.23 | 70 | 112.18 | 7.5 |
| | HSGFRP4 | 23.08 | 70 | 112.18 | 7 |
| | HSGFRP5 | 17.44 | 70 | 80.13 | 7.5 |
| | *Average* | *22.37* | *66* | *99.36* | *7.9* |

*Table 3. Experimental Results of all Mechanical Properties test*
*3. táblázat Az összes mechanikai vizsgálat eredménye*

The average values of the above results are summarized in *Table 4* below

| Samples | Tensile strength (MPa) | Impact energy (J) | Flexural strength (MPa) | Water absorption (%) |
|---|---|---|---|---|
| **GFRP** | 43.332 | 10.2 | 112.18 | 0.9447 |
| **HFRP** | 16.282 | 7.5 | 51.282 | 15.3979 |
| **SFRP** | 18.77 | 6.1 | 54.486 | 7.5829 |
| **HSFRP** | 22.82 | 7.8 | 44.87 | 8.7531 |
| **HGFRP** | 22.41 | 7.3 | 76.924 | 5.0827 |
| **SGFRP** | 19.87 | 5.7 | 105.77 | 2.8599 |
| **HSGFRP** | 22.894 | 7.9 | 105.77 | 3.4864 |

*Table 4 Summary for average mechanical properties*
*4. táblázat Mechanikai vizsgálatok átlagainak összefoglalója*

### 3.1 Tensile strength

*Fig. 4* demonstrates that the tensile strength of sisal fiber reinforced plastics (SFRP) outperforms that of hair fiber reinforced plastics (HFRP). This difference is attributed to the high water-absorption nature of hair fiber and the comparatively better water uptake of sisal fiber. Despite hair fiber exhibiting exceptional tensile strength per strand, the presence of voids and discontinuities resulting from its high water-absorption leads to the reduced tensile strength of HFRP. Additionally, factors such as hair fiber length and orientation further contribute to the weakening of HFRP.

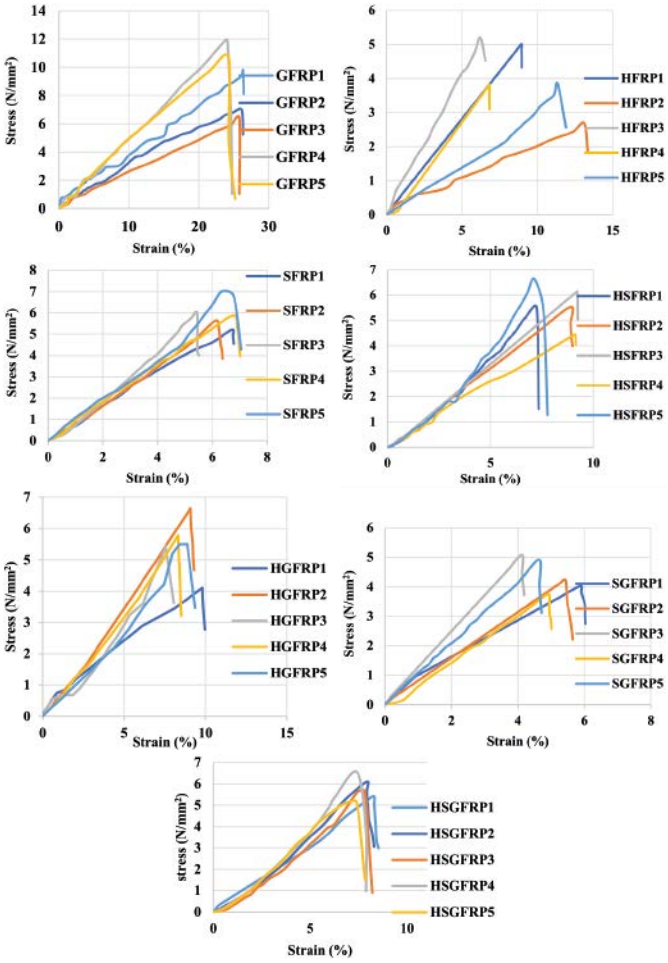


*Fig. 4 Stress-Strain relation of the composites*
*4. ábra Kompozitok feszültség-fajlagos alakváltozás összefüggése*

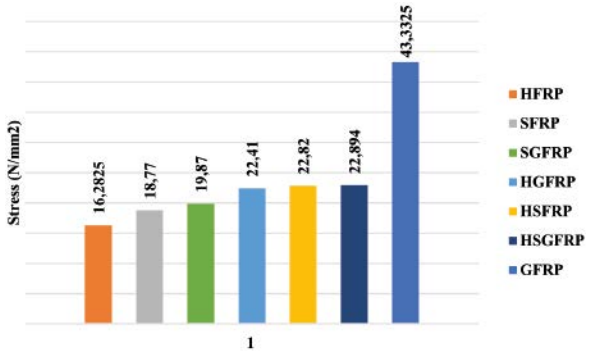


*Fig. 5 Average Tensile Strength of the Materials*
*5. ábra Anyagok átlagos húzószilárdsága*

The average values for tensile strength of each sample are summarized as in *Fig. 5* Hair/sisal/glass fiber reinforced plastics (HSGFRP) still exhibit the highest tensile strength compared to other fiber reinforced composite materials. However, it only satisfies 53% of the tensile strength of glass fiber reinforced plastics (GFRP). This aligns with the research objectives aimed at achieving intermediate strength for HSGFRP between GFRP and other natural and hybrid fiber reinforced composite materials.

### 3.2 Flexural strength

From *Fig. 6*, it is evident that the bending strength of sisal fiber reinforced plastics (SFRP) remains higher than that of hair fiber reinforced plastics (HFRP). This difference is attributed to the poor natural conduct of hair fiber compared to sisal fiber. The inherent shortcomings of hair fiber contribute to the formation of numerous discontinuities within the composite, leading to stress concentration and ultimately resulting in poor strength and premature failure under stress.

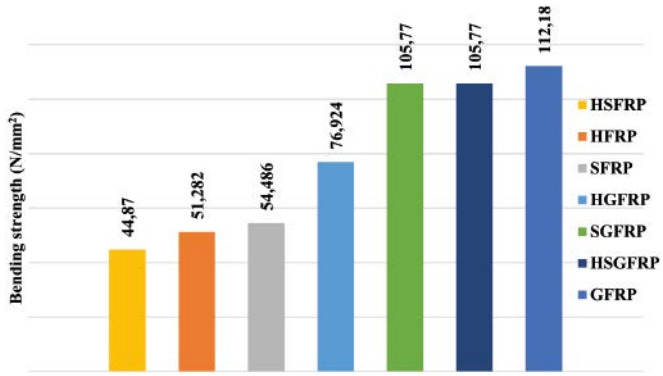


*Fig. 6 Flexural strength of the composite*
*6. ábra Kompozit hajlító-húzószilárdsága*

Interestingly, the combination of hair and sisal fiber reinforced plastics (HSFRP) exhibits significantly lower flexural strength compared to both sisal and hair fiber reinforced composites. This decrease in strength can be attributed to the cumulative negative effects of the two natural reinforcements. Moreover, HSGFRP satisfies 94% of the flexural strength of glass fiber reinforced plastics (GFRP). In summary, HSGFRP achieves a remarkable 94% of the flexural strength of GFRP.

### 3.3 Impact strength

*Fig. 4* shows that, hair fiber reinforced plastics (HFRP) exhibits higher impact stress absorption compared to SFRP materials. This can be attributed to the good ductility nature of human hair, aligning with one of the objectives set at the beginning for including hair fiber as a reinforcement. Impact strength typically increases with the percentage weight of reinforcement until reaching an optimum limit, as depicted in the graph. The rise in impact strength is primarily attributed to the contribution of hair fiber.

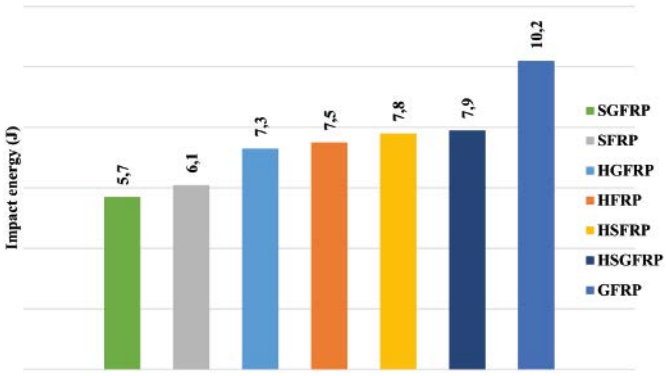


*Fig. 4. Impact strength of the composites*
*4. ábra Kompozitok ütőmunkája*

However, the addition of glass fiber has a negative effect on both HFRP and SFRP. This reversal is due to the absence of hair fiber, indicating that the inclusion of hair fiber up to its optimum point enhances impact strength. The impact strength of the required hybrid material (HSGFRP) remains satisfactory, primarily due to the presence of hair fiber.

In conclusion, hair/sisal/glass fiber reinforced polyester plastics (HSGFRP) fulfills approximately 77% of the impact strength of glass fiber reinforced polyester plastics (GFRP).

### 3.4 Water absorption

As depicted in *Fig. 5*, glass fiber reinforced composite has good water absorption, while hair fiber reinforced plastics (HFRP) shows the poorest behavior. Addition of glass fiber improves water absorption for both hair and sisal composites. Hair/sisal/glass fiber reinforced plastics (HSGFRP) exhibits a moderate absorption, 22% higher than sisal/glass composite, mainly due to hair fiber inclusion. Overall, HSGFRP displays favorable water absorption properties.

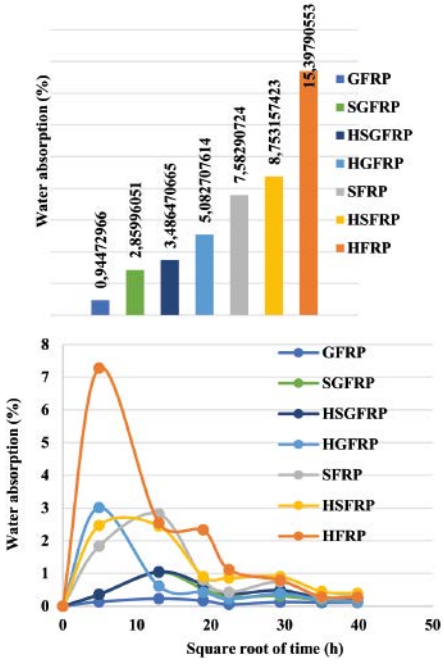


*Fig. 5 Water Absorption Test Results of the Samples*
*5. ábra Minták vízfelvétel vizsgálatainak eredménye*

## 4. Conclusions

The conclusions drawn from the study indicate that sisal fiber reinforced composite exhibits higher tensile and flexural strength but lower impact strength compared to hair fiber reinforced composite. The hair/sisal/glass fiber reinforced polyester plastics (HSGFRP) achieves 53% of the tensile, 94% of the flexural, and 77% of the impact strength of glass fiber reinforced Plastics (GFRP). The water absorption property of HSGFRP falls in the moderate range, following closely behind glass and glass/sisal fiber reinforced materials.

The addition of glass fiber enhances water absorption, tensile, and flexural strength but reduces impact strength in both hair and sisal fiber reinforced plastics. Overall, HSGFRP exhibits good mechanical properties compared to other hybrid fiber reinforced composites. However, there remains a notable gap, especially in tensile strength, between HSGFRP and GFRP.

## Acknowledgments

I extend my heartfelt gratitude to God for guiding me throughout my journey. Special thanks to my advisor, Dr. Abraham D., for his invaluable support and guidance. My family, especially my older brother, deserves recognition for shaping my life. Thanks to all friends, colleagues, and departments for their contributions. Lastly, I'm grateful to Mizan-Tepi University for sponsorship.

### References

[1] P. Srivastava, C. Kumar Garg, and S. Sinha, "The Influence of Chemical Treatment on the Mechanical Behaviour of hair Fibre-Reinforced Composites," 2018. [Online]. Available: www.sciencedirect.comwww.materialstoday.com/proceedings2214-7853

[2] K. John and S. V. Naidu, "Effect of fiber content and fiber treatment on flexural properties of sisal fiber/glass fiber hybrid composites," J. Reinf. Plast. Compos., vol. 23, no. 15, pp. 1601–1605, 2004, https://doi.org/10.1177/0731684404039799

[3] S. Koppula, A. K. Kaviti, and K. K. Namala, "Experimental Investigation of Fibre Reinforced Composite Materials under Impact Load," in IOP Conference Series: Materials Science and Engineering, Institute of Physics Publishing, Apr. 2018. https://doi.org/10.1088/1757-899X/330/1/012047

[4] S.V.N.V. Naga Prasad Naidu, G. Ramachandra Reddy, M. Ashok Kumar, M.Mohan Reddy, P. Noorunnisha Khanam, "Compressive & impact properties of sisal/glass fiber reinforced hybrid composites," Int. J. Fiber Text. Res. 2011;, vol. 1, no. 1, pp. 11–14, 2011.

[5] K. John and S. Venkata Naidu, "Sisal fiber/glass fiber hybrid composites: The impact and compressive properties," J. Reinf. Plast. Compos., vol. 23, no. 12, pp. 1253–1258, 2004, https://doi.org/10.1177/0731684404035270

[6] D. Senthilnathan, A. Gnanavel Babu, G. B. Bhaskar #, and K. Gopinath, "Characterization of Glass Fibre – Coconut Coir– Human Hair Hybrid Composites," vol. 6, no. 1, pp. 75–82, 2014.

[7] B. P. Nanda and A. Satapathy, "Processing and characterization of epoxy composites reinforced with short human hair," in IOP Conference Series: Materials Science and Engineering, Institute of Physics Publishing, Mar. 2017. https://doi.org/10.1088/1757-899X/178/1/012012

[8] N. Bheel, P. Awoyera, O. Aluko, S. Mahro, A. Viloria, and C. A. S. Sierra, "Sustainable composite development: Novel use of human hair as fiber in concrete," Case Stud. Constr. Mater., vol. 13, Dec. 2020, https://doi.org/10.1016/j.cscm.2020.e00412

[9] K. Karthikeyan, B. Prabhakaran, N. Manikandan, and K. Chandramohan, "Performance study of human hair fiber reinforced composite for the substitution of aluminium alloy piston," www.tjprc.org SCOPUS Index. J. Ed., no. Special Issue, pp. 123–127, 2018, [Online]. Available: www.tjprc.org

[10] R. K. Bhoyar, R. P. Kothe, S. Gillarkar, S. Chacherkar, R. Barve, and P. Mude, "Studies on Mechanical Behavior of Sisal Fiber and Human Hair Hybrid Sandwich Composites," Int. Res. J. Eng. Technol., 2020, [Online]. Available: www.irjet.net

[11] S. L. Fávaro, T. A. Ganzerli, A. G. V. de Carvalho Neto, O. R. R. F. da Silva, and E. Radovanovic, "Chemical, morphological and mechanical analysis of sisal fiber-reinforced recycled high-density polyethylene composites," Express Polym. Lett., vol. 4, no. 8, pp. 465–473, Aug. 2010, https://doi.org/10.3144/expresspolymlett.2010.59

[12] M. Kumaresan, S. Sathish, and N. Karthi, "Effect of fiber orientation on mechanical properties of sisal fiber reinforced epoxy composites," J. Appl. Sci. Eng., vol. 18, no. 3, pp. 289–294, 2015, https://doi.org/10.6180/jase.2015.18.3.09

[13] G. Rajesh, A. V. Ratna Prasad, and A. Gupta, "Mechanical and degradation properties of successive alkali treated completely biodegradable sisal fiber reinforced poly lactic acid composites," J. Reinf. Plast. Compos., vol. 34, no. 12, pp. 951–961, Jun. 2015, https://doi.org/10.1177/0731684415584784

[14] M. G. Prasad et al., "Investigation of Mechanical Properties of Sisal Fiber Reinforced Polymer Composites," Adv. J. Grad. Res., vol. 1, no. 1, pp. 40–48, Feb. 2017, https://doi.org/10.21467/ajgr.1.1.40-48

[15] P. Srivastava and S. Sinha, "Effect of surface treatment on hair fiber as reinforcement of HDPE composites: Mechanical properties and water absorption kinetics," Korean J. Chem. Eng., vol. 35, no. 5, pp. 1209–1218, May 2018, https://doi.org/10.1007/s11814-018-0011-2

[16] S. Arumugam et al., "Investigations on the Mechanical properties of glass fiber/sisal fiber/chitosan reinforced hybrid polymer sandwich composite scaffolds for bone fracture fixation applications," Polymers (Basel)., vol. 12, no. 7, pp. 1–19, Jul. 2020, https://doi.org/10.3390/polym12071501

[17] S. Dinesh, C. Elanchezhian, B. Vijayaramnath, A. Adinarayanan, and S. Guru Anantha Raman, "Evaluation of mechanical behavior for animal fiber Reinforced hybrid fiber composite for marine application," in IOP Conference Series: Materials Science and Engineering, IOP Publishing Ltd, Sep. 2020. https://doi.org/10.1088/1757-899X/912/5/052012

[18] I. D. Ibrahim, T. Jamiru, R. E. Sadiku, W. K. Kupolati, and S. C. Agwuncha, "Dependency of the Mechanical Properties of Sisal Fiber Reinforced Recycled Polypropylene Composites on Fiber Surface Treatment, Fiber Content and Nanoclay," J. Polym. Environ., vol. 25, no. 2, pp. 427–434, Jun. 2017, https://doi.org/10.1007/s10924-016-0823-2

Ref.:
**Belay**, Fikadu – **Debebe**, Abreham: *Characterization of hair-sisal-glass fibre polyester hybrid composite materials*
Építőanyag – Journal of Silicate Based and Composite Materials, Vol. 77, No. 1 (2025), 4–10 p.
https://doi.org/10.14382/epitoanyag-jsbcm.2025.1

## Öt szövetség együtt a hazai építőanyag-ipar jövőjéért – Megalakult a Szilikátipari Egyeztető Fórum


2025. június 12-én megalakult a Szilikátipari Egyeztető Fórum (SzEF), amely az építőanyag-gyártáshoz kapcsolódó szövetségek közötti szakmai együttműködést és közös fellépést hivatott erősíteni. Az alapító tagok: a Magyar Cement-, Beton- és Mészipari Szövetség (CeMBeton), a Magyar Kerámia Szövetség (MKSZ), a Magyar Építőanyag és Építési Termék Szövetség (MÉASZ), a Magyar Tégla és Tetőcserép Szövetség (MATÉSZ), valamint a Szilikátipari Tudományos Egyesület (SZTE).

A fórum célja, hogy a szövetségek közösen lépjenek fel az iparágat érintő legfontosabb szakpolitikai és gazdasági kérdésekben, összehangolják érdekképviseleti munkájukat, és közös állásfoglalásokkal, javaslatokkal segítsék az ágazat fenntartható fejlődését.

A CeMBeton tagsága a cement-, beton- és mészipariban működő vállalkozásokból, építéskémiai-, valamint laborcégekből áll, amelyek a modern építőipar szerkezeti alapját adják. A szövetség elkötelezett a körforgásos gazdaság, az alacsony karbonlábnyomú technológiák, az oktatási és a szabályozási környezet fejlesztése mellett.

A MATÉSZ a hazai tégla és tetőcserép gyártók szakmai érdekképviseleti szervezete. Fő feladata a hazai tégla- és cserépipari cégek összefogásával az ágazati érdekek érvényesítése Magyarországon és az Európai Unióban. A Szövetség a termelés gazdasági, jogi feltételeinek, a termékek minőségének javítása érdekében számos területen tevékenykedik.

A Magyar Építőanyag és Építési Termék Szövetség (MÉASZ) szakmai ernyőszövetségként fogja össze a hazai építőanyag-ipar öt szakszövetségét és számos további hazai gyártót. A MÉASZ tagjai a közvetlen működési környezetre vonatkozó érdekképviseleti munkán túl elkötelezettek mindazon ösztönzők és szabályozások kialakításában, amelyek innovatív és energiahatékony új építési beruházásokat, valamint minőségi épületkorszerűsítéseket, felújításokat eredményeznek. A Szövetség tagjai kulcsszerepet töltenek be a foglalkoztatás, a K+F és az oktatás terén az értékláncban.

A Magyar Kerámia Szövetség többek között a burkoló-, a szaniterkerámia-gyártó és a tűzállóanyag-ipari szereplők érdekeit is képviseli. E három szakterület nemcsak a lakó- és közösségi épületek komfortját határozza meg, hanem az építőanyag-ipar ipari hátterét is alakítja. A tűzálló kerámiák például elengedhetetlenek a cement- és üveggyártás magas hőmérsékletű technológiáihoz, így közvetve az építőanyag-gyártás értéklláncának alapját is képezik.

A Szilikátipari Tudományos Egyesület (SZTE) a hazai anyagtudományi kutatások és mérnöki tudás központi platformja, amely összeköti az ipart, a tudományos életet és az oktatást. Szerepe kulcsfontosságú az utánpótlás képzésében és az innováció előmozdításában.

A SzEF működése négy fő pillérre épül: szakmai tudásmegosztás, összehangolt érdekképviselet, szakember-utánpótlás biztosítása és az iparági innováció – különösen a zöld technológiák – előmozdítása.

Az együttműködés célja, hogy az építőanyag-ipar teljes spektrumát képviselő szövetségek közös hangon szólaljanak meg a legfontosabb ágazati kérdésekben, hozzájárulva ezzel a hazai építésgazdaság stabilitásához, fenntarthatóságához és nemzetgazdasági súlyának növekedéséhez.

Budapest, 2025. június 13.

# Impact of fire exposure on the rebar-concrete bond strength

**Ahmed Omer Hassan ALI** ▪ Budapest University of Technology and Economics, Budapest, Hungary
**Éva LUBLÓY** ▪ Budapest University of Technology and Economics, Budapest, Hungary
Érkezett: 2025. 01. 13. ▪ Received: 13. 01. 2025. ▪ https://doi.org/10.14382/epitoanyag-jsbcm.2025.2

**Ahmed Omer Hassan ALI**
MSc in Structural Engineering and a PhD candidate at the Budapest University of Technology and Economics. He is a Graduate Member of the Institution of Structural Engineers (IStructE) with research interests in fire resistance, progressive collapse, and the bond behavior between reinforcement and concrete. With experience as a Structural Engineer and Lecturer.

**Éva LUBLÓY**
is a civil engineer (Budapest University of Technology and Economics, Faculty of Civil Engineering, 2001), and a university professor at the Department of Construction Materials and Building Structures at BME. She is a Doctor of the Hungarian Academy of Sciences. Her main areas of interest are the behavior of reinforced concrete structures under fire exposure and the engineering lessons learned from fire damage.

**Abstract**
Structural fire resistance is a primary aspect of a passive fire engineering design measure that allows a structure to withstand intense fires. Generally, concrete structural elements perform well under these conditions due to their non-flammable nature. However, fire incidents require a deeper understanding of concrete behavior and structural mechanics to improve fire design. Structural elements exposed to fire and heat show reduced strength; this reduction must be evaluated to determine whether to demolish or repair a building based on its condition and capability to support future loads.
Evaluating the post-fire strength characteristics, including compressive, tensile, and bond strengths, is essential for determining the structure's safety. Prolonged exposure to high temperatures can degrade concrete properties, particularly the bond strength between rebar and concrete. This paper investigates the bond strength of materials after exposure to fire. The study explores the effects of temperatures ranging from 20 °C to 500 °C, following the ISO 834 fire curve, on compressive, tensile, and bond strengths. Cylindrical pull-out specimens were heated to specific temperatures and held for 2 hours. Afterward, they were cooled for one day before testing. The results indicate that bond strength decreases by approximately 72% at 500 °C, about twice the reduction observed in compressive and tensile strengths.
Keywords: bond, elevated temperature, pullout test, residual bond strength
Kulcsszavak: tapadás, magas hőmérséklet, kihúzóvizsgálat, maradó tapadószilárdság

## 1. Introduction

Structural fire resistance is a key aspect of fire safety, often regarded as a passive measure that allows a structure to withstand intense fires [1]. Concrete performs well in fire due to its incombustibility, but real-fire scenarios emphasize the need for a deeper understanding of concrete behavior and structural mechanics to improve fire design in reinforced concrete structures [2].

The bond between rebar and concrete is formed through adhesion, mechanical interlock, and friction [3]. Bond-mechanism, ensures that reinforced concrete acts as a composite material. Under normal temperatures, factors affecting bond strength are well understood, but quantifying their effects remains an active research area. Material properties, such as concrete strength, aggregate type, admixtures, and testing methods, significantly influence bond performance [4, 5].

Bond evaluation becomes more complex at elevated temperatures as the heating becomes dominant; the physical properties of concrete undergo significant changes due to temperature gradients [6]. Fire causes heat to penetrate the concrete, raising its temperature and leading to thermal expansion, moisture evaporation, pore pressure buildup, and mechanical property degradation [7]. This effect weakens the rebar-concrete bond [8], leading to endangering of the overall structural integrity. Structural engineering thus, must ensure these factors do not affect the structure's primary functions [7].

## 2. Literature review

Morley and Royle's [9] tested the four conditions of the stabilized temperature procedure, these tests indicate that specimens subjected to stress during the heating cycle demonstrate slightly greater strength than those not stressed, as shown in *Fig. 1*. Diederichs and Schneider [5] studied the impact of bar surface properties using plain rebar and two types of deformed bars. Their tests revealed significant bond strength deterioration in all specimens. Additionally, the tests showed that deformed rebar followed similar temperature-bond relationships as plain rebar but with improved performance, as shown in *Fig. 2*. The results also indicated that corroded plain rebar outperformed new, as-rolled rebar.

Haddad *et al.* created specimens with plain and fiber-reinforced concrete using three fiber types. Below 600 °C, fibers improved residual bond strength by preventing crack propagation and spalling. The best performance was seen in concrete with only Hooked Steel fibers, followed by a mix of hooked steel and brass-coated steel fibers, hooked steel and polypropylene, and Brass-coated steel fibers alone [10].

Xiao *et al.* studied specimens with high-strength rebar and concrete, finding a significant bond decline and increased peak slip beyond 400 °C [11]. Haddad and Shannis, using high-strength concrete with pozzolanic material replacing 10%, 15%, and 25% of cement, observed bond deterioration at 600 °C and 800 °C — up to 24% at 600 °C and 74% at 800 °C. However, using up to 25% natural pozzolana at temperatures up to 60 °C improved crack resistance and maintained bond strength without adverse effects [12].

Sharma *et al.* proposed a linear model based on test results to estimate the reduction in residual bond strength of normal-strength concrete at elevated temperatures [13]. Ergün *et al.* developed mathematical equations that focus on the impact of rebar properties, considering different steel grades (S220a,

S420a, S500a) [14]. Haddad *et al.* created an empirical model for high-strength concrete, examining the effects of various fiber types in the mix, including plain concrete, steel fibers (brass-coated or hooked), and high-modulus polypropylene fibers [10].

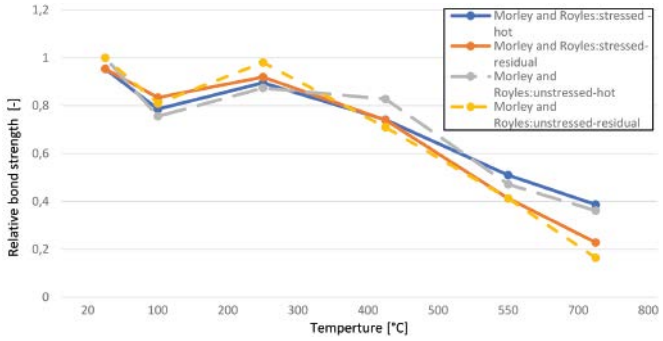


*Fig. 1 Relative bond strength response to elevated temperatures using the stabilized temperature method according to Morley and Royle's [9]*
*1. ábra A relatív tapadószilárdság alakulása emelkedett hőmérsékleten a Morley és Royle [9] által alkalmazott stabilizált hőmérséklet módszer szerint*

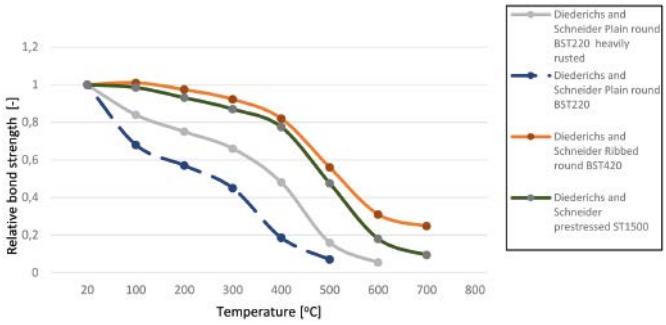


*Fig. 2 Influence of rebar rib characteristics on residual relative bond strength at elevated temperature [5]*
*2. ábra A betonacél bordáinak jellemzőinek hatása a magas hőmérsékleten maradó relatív tapadószilárdságra [5]*

## 3. Experimental program

The authors conducted an experimental study to examine the impact of high temperatures on bond, tensile, and compressive properties. The oven depicted in *Fig. 3* was used, and the ISO 834 fire curve in *Fig. 4* was followed. The temperature range varied from 20 °C to 500 °C.

*Fig. 3 Oven during the heating stage*
*3. ábra Kemence a felfűtési szakaszban*

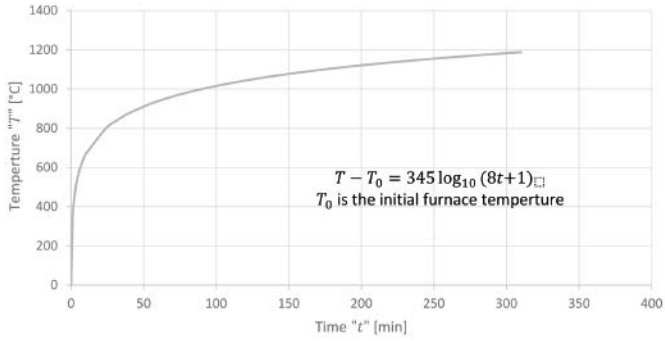


*Fig. 4 Heating rates adopted according to ISO 834 standard fire curve*
*4. ábra Az ISO 834 szabvány szerinti tűzgörbéhez alkalmazott felfűtés*

### 3.1 Concrete mixture

The mix compositions are given in *Table 1*. Type CEM I cement was adopted, quartz sand and gravel aggregate were used.

| Material | Type | Mass, kg/m³ |
|---|---|---|
| **Aggregate** | 0/4 mm | 780 |
| | 4/8 mm | 372 |
| | 8/16 mm | 706 |
| **Cement** | CEM I 52.5 | 350 |
| **Water** | - | 175 |

*Table 1 The concrete mixes.*
*1. táblázat Beton összetételek*

### 3.2 Test setup

Cylindrical pull-out specimens with a diameter of 120 mm and a height of 100 mm were prepared. The cylindrical shape allowed for uniform stress distribution during testing and consistent heating throughout the thermal cycles. The bonded length was 40 mm, while the unbonded length on both sides was 30 mm. Ribbed steel bars with a 12 mm diameter were used, and slip was measured with three linear variable differential transformers (LVDTs) at the loaded end of the bar, along with one LVDT at the free end. An automatic data acquisition system was used to record the data transmitted by the LVDTs. Details of the pull-out tests are shown in *Fig. 5*.

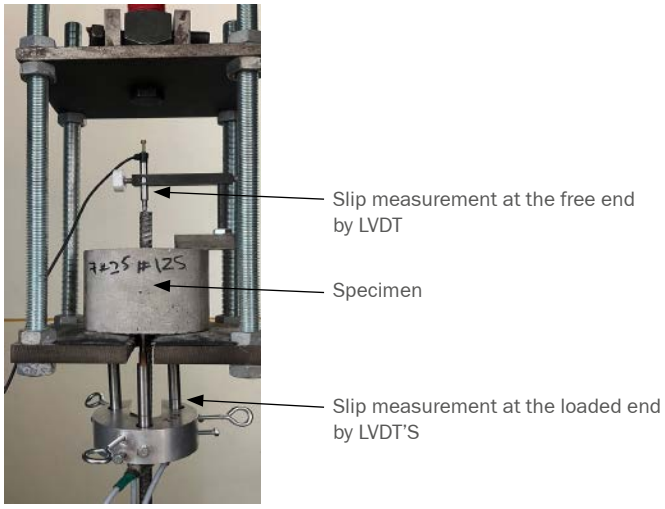


*Fig. 5 Test setup*
*5. ábra Kísérleti elrendezés*

### 3.3 Heating procedure

After demolding the specimens one-day post-casting, they were immersed in water for six days. On the test day, the specimens were heated to different temperatures (20 °C, 150 °C, 300 °C, 500 °C) and maintained at each temperature for two hours. After heating, the specimens were gradually cooled to laboratory temperature over one day. Subsequently, compressive strength on cylinder specimens was measured using a concrete compression testing machine, tensile strength was measured using the three-point flexural test, and pull-out tests were conducted.

## 4. Test results

### 4.1 Compressive strength

Compressive strength was measured after heating on 200x100 mm cylindrical specimens, as shown in *Fig. 6*. *Table 2* and *Fig. 7* show the measured compressive strength values and the relative residual compressive strength (the compressive strength ratio after heating to the compressive strength at 20 °C) of the concrete specimens as a function of the maximum temperature. At 500 °C, the deterioration reached 33%, exhibiting a nearly linear decline across the temperature range tested.

*Fig. 6 Compression strength test*
*6. ábra Nyomószilárdság vizsgálat*

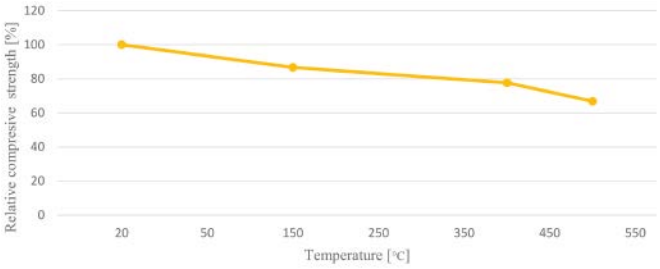


*Fig. 7 Residual compressive strength at elevated temperature*
*7. ábra Maradó nyomószilárdság magas hőmérsékleten*

| Temperature | 20 °C | 150 °C | 400 °C | 500 °C |
|---|---|---|---|---|
| **Compressive strength (N/mm²)** | 53.95 | 46.74 | 41.90 | 36.06* |
| **Residual compressive strength [%]** | 100.00 | 86.63 | 77.66 | 66.83 |
| **Tensile strength (N/mm²)** | 6.15 | 5.75 | 5.05 | 4.14 |
| **Residual tensile strength [%]** | 100.00 | 93.49 | 82.11 | 67.38 |
| **Bond strength (N/mm²)** | 20.97 | 20.88 | 10.42 | 5.92 |
| **Residual bond strength [%]** | 100.00 | 99.57 | 49.69 | 28.23 |

**The average of two specimens was taken as one of the specimens spalled.*

*Table 2 Measured strength at elevated temperature*
*2. táblázat Mért szilárdság magas hőmérsékleten*

### 4.2 Tensile strength

Tensile strength was measured after the heating procedure on 70x70x250 mm prism specimens, as shown in *Fig. 8*. *Table 2* and *Fig. 9* display the measured tensile strength values and the relative residual tensile strength (the ratio of tensile strength after heating to tensile strength at 20 °C). At 500 °C, the deterioration of the tensile strength reached 33%.

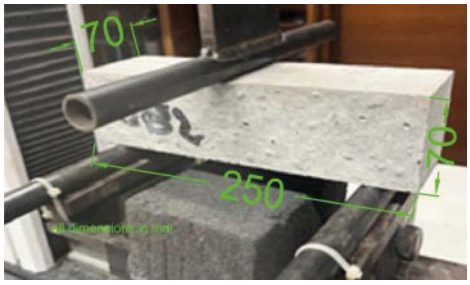


*Fig. 8 Flexural-tensile strength test*
*8. ábra Hajlító-húzószilárdság-vizsgálat*

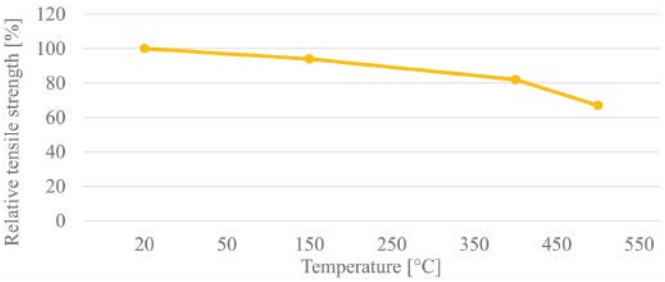


*Fig. 9 Residual tensile strength at elevated temperature*
*9. ábra Maradó szakítószilárdság emelt hőmérsékleten*

### 4.3 Bond strength

Bond strength was measured after the heating procedure on 120x100 mm cylindrical specimens, all exhibiting splitting failure, as shown in *Fig. 10*.

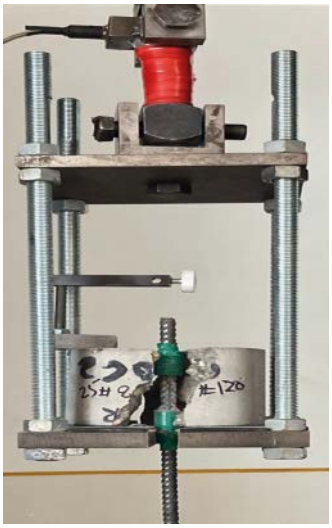

*Fig. 10 Splitting failure of pullout cylinder specimen*
*10. ábra Hengeres próbatest hasadási tönkremenetele kihúzó vizsgálatnál*

Since the bond length is less than 5 $d_s$, the applied load, F, was converted to average bond stress, $\tau_b$ the bonded length using the uniform bond stress approach as follows:

$$\tau_b = \frac{F}{\pi d_s l_b}$$

Where:
$F$ is the applied tensile force on the rebar,
$d_s$ is the diameter of the rebar, and
$l_b$ is the bonded length, which is 40 mm in the present study.

*Table 2* and *Fig. 11* display the measured bond strength values and the relative residual bond strength (the ratio of bond strength after heating to bond strength at 20 °C); at 500 °C, the deterioration of the bond strength reached approximately 72%.

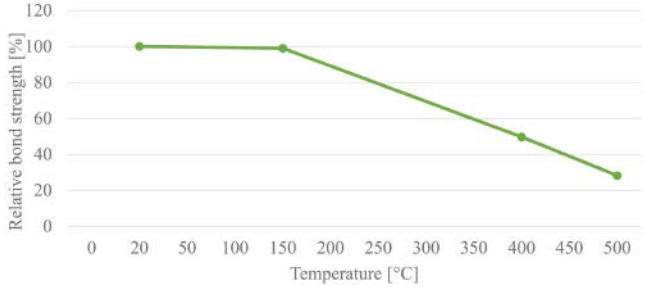


*Fig. 11 Residual bond strength at elevated temperature*
*11. ábra Maradó tapadószilárdság magas hőmérsékleten*

The following bilinear equation describes the degradation of bond strength:

$$Residual\ bond\ strength = \begin{cases} -0.0033 \cdot T + 100.066 \ \ if\ T \leq 150°C \\ -0.2039 \cdot T + 130.155 \ \ if\ 150°C < T \leqq 500°C \end{cases}$$

### 4.4 Bond-slip curve at elevated temperature

The stress-slip relationships for the pull-out failure mode and splitting failure are illustrated in *Fig. 12.* As depicted in *Fig. 12,* elevated temperatures cause deterioration of bond strength, resulting in a reduction in the ascending branch.

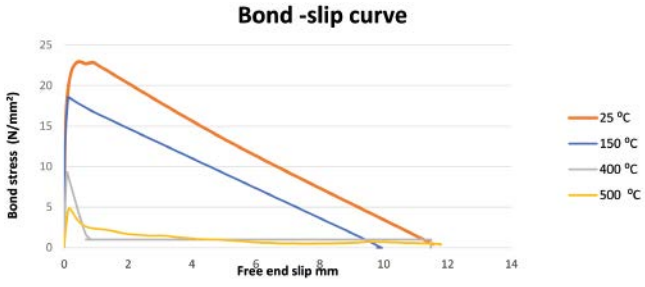


*Fig. 12 Bond-slip curve at elevated temperatures*
*12. ábra Tapadás–csúszás görbe magas hőmérsékleten*

## 5. Conclusion

This paper examines the effects of rising temperatures according to the ISO 843 standard fire curve, focusing on a temperature range between 25 °C and 500 °C. We investigated the impact on bond, compressive, and tensile strength using pullout, cylinder tests, and prism specimens. After heating the specimens and maintaining the target temperature for 2 hours, all tests were conducted in their residual state after a cooling period of one day. Based on our findings, we can conclude that:

I. As the temperature rises, the compressive, tensile, and bond strengths decrease across all examined temperatures. However, the decline in bond strength becomes more pronounced than the reduction in compressive and tensile strengths at temperatures of 400 °C and above.
II. At 500 °C, the deterioration of compressive strength reached 33%, exhibiting a linear decline across the temperature range tested.
III. At 500 °C, the deterioration of the tensile strength reached 33%.
IV. Half of the bond capacity was degraded when the temperature reached 400 °C.
V. The residual bond strength at 500 °C is approximately 28.23% of the reference capacity under laboratory conditions. The bond showed a significant decline of around 72%, twice the deterioration observed in tensile and compressive strength at elevated temperatures.
VI. The degradation of bond strength can be expressed using the following equations:

$$Residual\ bond\ strength = \begin{cases} -0.0033 \cdot T + 100.066 \ \ if\ T \leq 150°C \\ -0.2039 \cdot T + 130.155 \ \ if\ 150°C < T \leqq 500°C \end{cases}$$

### References

[1] The Institution of Structural Engineers, Introduction to structural fire engineering, The Institution of Structural Engineer, 2020.
[2] The International Federation for Structural Concrete (fib), Fire design of concrete structures structural behaviour and assessment, The International Federation for Structural Concrete (fib), 2008.
[3] Bond of reinforcment in concrete, International federation of structural concrete fib, 2000.
[4] ACI committee 408, Bond and Development of Straight Reinforcing Bars in Tension, American Concrete Institut, 2003.
[5] U. Diederichs and U. Schneider, "Bond strength at high temperatures," Magazine of Concrete Research, vol. 33, no. 115, pp. 75-84, 1981.
[6] K. Abuhishmeh, H. H. Jalali, M. Ebrahimi, M. .Soltanianfard and J. S. C. Cesar Ortiz Correa, "Behavior of high strength reinforcing steel rebars after high temperature exposure: Tensile properties and bond behavior using pull-out and end beam tests," Engineering Structures, vol. 305, 2024.
[7] The international Federation of structural concrete , Fire design of concrete structures , materials , structures and modeling, 2007.
[8] É. Lublóy and VHlavička, "Bond after fire," Construction and Building Materials, vol. 132, pp. 210-218, 2017.
[9] P. D. Morley and R. Royles, "The Influence of High Temperature on the Bond in Reinforced Concrete," Fire Safety Journal, vol. 2, pp. 243 - 255, 1980.
[10] R. Alsaleh and N. Al-Akhras, "Effect of elevated temperature on bond between steel reinforcement and fiber reinforced concrete," Fire Safety Journal, vol. 43, p. 334–343, 2008.
[11] J. Xiao, Y. Hou and Z. Huang, "Beam test on bond behavior between high-grade rebar and high-strength concrete after elevated temperatures," Fire Safety Journal, vol. 69, pp. 23-35, 2014.
[12] R. H. Haddad and L. G. Shannis, "Post-fire behavior of bond between high strength pozzolanic concrete and reinforcing steel," Construction and Building Materials, vol. 18, p. 425–435, 2004.
[13] A. Sharmaa, J. Bošnjakb and S. Bessertc, "Experimental investigations on residual bond performance in concrete subjected to elevated temperature," Engineering Structures, vol. 187, pp. 384-395, 2019.
[14] A. Ergün, G. Kürklü and M. S. Baspınar, "The effects of material properties on bond strength between reinforcing bar and concrete exposed to high temperature," Construction and Building Materials, vol. 112, p. 691–698, 2016.

Ref.:
**Ali**, Ahmed Omer Hassan – **Lublóy**, Éva: *Impact of fire exposure on the rebar-concrete bond strength*
Építőanyag – Journal of Silicate Based and Composite Materials, Vol. 77, No. 1 (2025), 11–14 p.
https://doi.org/10.14382/epitoanyag-jsbcm.2025.2

# Thermogravimetry and thermodilatometry as auxiliary analyses for dynamical thermomechanical analysis of clays

**Tibor KOVÁCS** ▪ Department of Physics, Faculty of Natural Sciences and Informatics, Constantine the Philosopher University in Nitra, Slovakia ▪ tibor.kovacs@ukf.sk
**Igor ŠTUBŇA** ▪ Department of Physics, Faculty of Natural Sciences and Informatics, Constantine the Philosopher University in Nitra, Slovakia ▪ igor.c.stubna@gmail.com
**Anton TRNÍK** ▪ Department of Physics, Faculty of Natural Sciences and Informatics, Constantine the Philosopher University in Nitra, Slovakia ▪ atrnik@ukf.sk
**Libor VOZÁR** ▪ Department of Physics, Faculty of Natural Sciences and Informatics, Constantine the Philosopher University in Nitra, Slovakia ▪ lvozar@ukf.sk
Érkezett: 2025. 01. 18. ▪ Received: 18. 01. 2025. ▪ https://doi.org/10.14382/epitoanyag-jsbcm.2025.3

**Abstract**
The natural illitic clay was mixed with powder calcite (22 wt.% in the dry mixture), distilled water, and 3% solution of polyvinyl alcohol to obtain a plastic mass for samples. To determine the correct temperature dependence of Young's modulus, thermogravimetry (TG), thermodilatometry (TDA), and impulse excitation technique (IET) have to be performed in the same temperature regime. The effect of the size of TDA sample on Young's modulus was negligible. Contrary to the TDA sample, the form of the TG sample had a significant effect. When results from a small TG powder sample are substituted into the formula for Young's modulus, relative error up to 10% can result in the temperature region in which changes of some mineral components occur. In this study, we showed the importance of using compact samples with the same cross-section for TG, TDA, and IET in order to obtain correct values of Young's modulus during thermal treatment of the illitic clay.
Keywords: thermal analysis, sample size, thermogravimetry, thermodilatometry, Young's modulus
Kulcsszavak: termikus analízis, mintaméret, termogravimetria, termodilatometria, Young-modulus

**Tibor KOVÁCS**
PhD. student at Department of Physics, Faculty of Natural Sciences and Informatics, Constantine the Philosopher University in Nitra, Nitra, Slovakia. Field of research: Mechanical and thermophysical properties of anorthite ceramic materials.

**Igor ŠTUBŇA**
Associate professor at Department of Physics, Faculty of Natural Sciences and Informatics, Constantine the Philosopher University in Nitra, Nitra, Slovakia. Field of research: Mechanical and thermophysical properties of the kaoline-based and illite-based ceramics, firing of ceramics, measurement of the dynamical mechanical properties (sound velocity, moduli of elasticity).

**Anton TRNÍK**
Associate professor at Department of Physics, Faculty of Natural Sciences and Informatics, Constantine the Philosopher University in Nitra, Nitra, Slovakia. Field of research: Mechanical and thermophysical properties of the kaoline-based and illite-based ceramics, thermal analysis, measurement of the dynamical mechanical properties (sound velocity, moduli of elasticity).

**Libor VOZÁR**
Professor at Department of Physics, Faculty of Natural Sciences and Informatics, Constantine the Philosopher University in Nitra, Nitra, Slovakia. Field of research: Thermophysical properties of ceramic materials, thermal analysis, measurements of the thermal diffusivity and conductivity, and heat capacity.

## 1. Introduction

It is important to understand how mechanical properties of traditional ceramics behave not only during firing of the product, but also when the product is in fire or when it is used in a work environment at elevated temperatures. Firing of clays with a high content of kaolinite and/or illite transforms a raw (unfired) body into ceramic products. The raw body exhibits changes during heating that result from dehydration, dehydroxylation, high-temperature reactions, sintering, and transitions of quartz [1, 2], which affecting the properties of the final fired body. To study these changes, methods of thermal analyses are used. The most commonly used ones are differential thermal analysis (DTA), differential scanning calorimetry (DSC), thermogravimetry (TG), and thermodilatometry (TDA). When ceramic materials are intended to be used in high-temperature environment, e.g. at firing, it is also important to know the mechanical properties of ceramic material, as well as changes caused by the heat. The suitable method for this purpose is the dynamical thermomechanical analysis (D-TMA) [3, 4].

In DTA, the sample of interest and the reference sample undergo identical thermal cycles, and the temperature difference between the samples is recorded and plotted against time or against temperature. Changes in the sample, either exothermic or endothermic, can be detected relative to the inert reference sample. Thus, a DTA curve provides data on dehydration, dehydroxylation, and high-temperature reactions. The ideal reference material is a substance with no thermal events over the temperature range of interest. In DTA, alumina ($Al_2O_3$) powder is used as the reference material for the analysis of inorganic compounds.

In TG, the mass of a sample is monitored also against time or temperature. This technique is used to characterize clay materials that experience mass loss related to dehydration, dehydroxylation and decomposition. D-TMA is based (in most cases) on measuring the resonant frequency of the vibrating sample during its heating/cooling or heating at constant temperature.

DTA and TG are often performed simultaneously in the DTA/TG analyzer, in which small powder samples (tens of mg in modern analyzers) are used. For some cases, it is preferable to measure compact samples of sizes and masses comparable to samples used in TDA or D-TMA. It is known that the sample size plays a significant role in thermal analyses. For example, DTA and DTG peaks occur at higher temperatures for larger samples. In large samples comparable to some industrial bodies, dehydration and dehydroxylation take place simultaneously – dehydroxylation begins on the surface at ~420 °C and dehydration finishes in the middle even at such slow heating rate as 3 °C/min [5].

Samples for DTA/TG, D-TMA, and TDA had the same cross-section [4, 6, 7]. The sample for DTA/TG had a shape of cylinder of dimensions Ø10×20 mm$^2$ or prism 10×10×20 mm$^3$

both with an opening Ø3×10 mm² for a thermocouple. The reference sample was made from a pressed alumina powder and had the same shape and dimensions as the measured sample. A similar sample for DTA was shortly described in [8], where is stated that this sample gives sharper DTA peaks than a powder sample in a crucible.

Young's modulus can be measured only indirectly. To determine its value, some physical quantities have to be measured and substituted into a relevant formula. The sonic resonance method (SRM) or impulse excitation technique (IET) [4, 9–11], which are non-destructive and sufficiently sensitive, can be successfully used for D-TMA if an appropriate temperature regime is applied. A flexural vibration of the measured cylindrical or prismatic sample is mostly used because of the simplicity and reliability of its excitation and measurement at elevated temperatures. For the flexural vibration, Young's modulus $E$ may be calculated using formula [10–12]

$$E = \left(K\frac{l^2 f_0}{d}\right)^2 \frac{m}{V}T \tag{1}$$

where $f_0$ is the resonant frequency of the fundamental mode, $m$ is the mass of the sample and $V$ is its volume, $l$ is the length, and $d$ is the dimension of the sample in the vibration plane (i.e. diameter or thickness). The values of the constant $K$ are:
$K$ = 1.12336 for a circular cross-section and the fundamental resonant frequency,
$K$ = 0.97286 for a square cross-section and the fundamental resonant frequency.

The correction coefficient $T = 1$ if $l/d \geq 20$. If not, $T$ must be calculated from the formulae given in [10, 11] or can be found in tables in [12]. To obtain $T$, Poisson's ratio of the measured material must be known. The value 0.2 can be considered for ceramics [4, 9]. In practice, the ratio of $l/d$ varies between 10 and 15. Using the values of $T$ from [12], the sufficiently accurate relationship between $T$ and $l/d$ for the actual temperature $t$ can be written as

$$T(t) = 0.9859 + 0.609\frac{d(t)}{l(t)} \text{ for a circular cross section} \tag{2a}$$

$$T(t) = 0.9704 + 0.950\frac{d(t)}{l(t)} \text{ for a square cross section} \tag{2b}$$

During heating of ceramic material, the mass, length and cross-section alter their values depending on the temperature. Young's modulus is also a function of the resonance frequency $f_0$. Therefore, three thermal analyses (TG, TDA, and D-TMA) must be performed to obtain the correct values of Young's modulus. Calculation of Young's modulus can be simplified if TG and TDA are omitted. This necessarily leads to an error, which can reach 7.5% [6]. It follows that TG and TDA are auxiliary analyses that help obtain more exact values of Young's modulus.

The length and diameter/thickness of the sample can be written as $l(t) = l_0 + \Delta l(t)$ and $d(t) = d_0 + \Delta d(t)$, where $l_0$ and $d_0$ are their values at the room temperature and $\Delta l(t)$, $\Delta d(t)$ are contributions from the thermal expansion measured by dilatometer. Since ceramic material is considered isotropic, $\Delta l(t)/l_0 = \Delta d(t)/d_0 = \varepsilon$. The term $d(t)/l(t)$ in *Eq. (2a)* and *(2b)* can be expressed as

$$\frac{d(t)}{l(t)} = \frac{d_0\left(1+\frac{\Delta d(t)}{d_0}\right)}{l_0\left(1+\frac{\Delta l(t)}{l_0}\right)} = \frac{d_0(1+\varepsilon)}{l_0(1+\varepsilon)} = \frac{d_0}{l_0} \tag{3}$$

Similarly, $m(t) = m_0 + \Delta m(t)$ is the mass of the sample at the temperature $t$, where $\Delta m(t)$ is the mass loss measured with a TG analyzer. Then *Eq. (1)* using *Eq. (2a)*, *Eq. (2b)* and *Eq. (3)* can be written as

$$E(t) = 1.6067\frac{m_0\left(1+\frac{\Delta m(t)}{m_0}\right)l_0^3 f(t)^2}{d_0^4\left(1+\frac{\Delta l(t)}{l_0}\right)}\left(0.9859 + 0.609\frac{d_0}{l_0}\right) \tag{4a}$$

for a circular cross-section and

$$E(t) = 0.9465\frac{m_0\left(1+\frac{\Delta m(t)}{m_0}\right)l_0^3 f(t)^2}{d_0^4\left(1+\frac{\Delta l(t)}{l_0}\right)}\left(0.9704 + 0.950\frac{d_0}{l_0}\right) \tag{4b}$$

for a rectangular cross-section. Usually, if the investigated ceramic samples are fired at a temperature above 800 °C, its mass is constant, i.e. $\Delta m(t) = 0$ and *Eq. (4a)* and *(4b)* can be simplified.

The aim of the article is to assess the differences between the results of Young's modulus when powder samples or compact samples are used in thermal analyses TG and TDA. Also, the importance of using uniform samples across the analyses in order to generate results suitable for determination of their elastic constants during their thermal treatment is shown.

## 2. Experimental

Natural clay from Füzérradvány (north-eastern Hungary) was ground and sieved to get a powder, which was then mixed with powder calcite ($CaCO_3$) in the mass ratio $m_{clay}/m_{calcite}$ = 78/22. This mixture was mixed with the distilled water and 3% solution of polyvinyl alcohol to obtain a plastic mass from which prismatic samples were pressed. Their dimensions after drying were 9×9×120 mm³. Thermal analyses were performed as follows:

- TG for small powder samples (40 mg) in alumina crucible on the TG/SDTA Mettler-Toledo analyzer.
- TG for compact samples 8×8×15 mm³ on the DTA/TG analyzer Derivatograph 1000 [13]. The sample had a hole Ø3×6 mm² for alumina double capillary rod with thermocouple. The reference sample of the same shape and dimensions made from pressed alumina powder was used for DTA.
- TDA for samples 8×8×20 mm³ and 4×4×20 mm³ on the dilatometer Netzsch DIL 402 C.
- D-TMA for sample 8×8×110 mm³ on the IET apparatus [14].
- The heating rate for all analyses was 5 °C/min.
- The temperature interval for all analyses was from room temperature up to 1100 °C.

The analyzer Derivatograph performs simultaneously TG and DTA. Although DTA does not give any quantity for Eq. (3a) or Eq, (3b), DTA helps to get a better picture of the processes in the studied sample.

The result of $\Delta l(t)/l_0$ from TDA, $\Delta m(t)/m_0$ from TG, and resonant frequency from D-TMA were substituted into Eq. (4b) to determine the thermal behavior of Young's modulus.

## 3. Results and discussion

Results of TG are pictured in *Fig. 1*. The main processes are mirrored here – removal of the physically bound water (up to 200 °C), dehydroxylation of illite/smectite (420 °C – 650 °C) and decomposition of calcite above 600 °C, which has a steep decline and is sharply ended. The curves differ as commonly known for TG when samples of different mass are used: the development and termination of processes are shifted to higher temperatures for larger samples.

An example illustrating how the different mass losses influence Young's modulus at 750 °C is as follows (see *Eq. (5)*). When only the relative mass losses of the compact sample (6%) and powder sample (14%) are substituted in *Eq. (4b)*, the ratio of Young's moduli is

$$\frac{E_{TG\ of\ powder\ sample}}{E_{TG\ of\ compact\ sample}} = \frac{1-0.14}{1-0.06} = 0.915\,. \qquad (5)$$

This result implies, that the use of TG results obtained using small powder samples can lead to a relative error of ~10%.

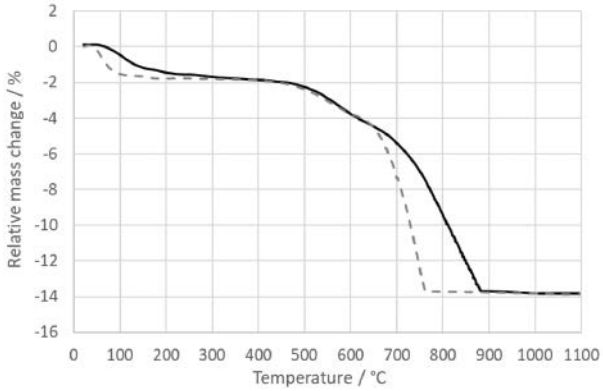


*Fig. 1* *The curves of relative mass change for a 40 mg powder sample (dashed line) and a 3 g compact sample (solid line)*
*1. ábra* *A relatív tömegváltozás görbéi egy 40 mg-os porminta (szaggatott vonal) és egy 3 g-os tömör minta (folytonos vonal) esetén*

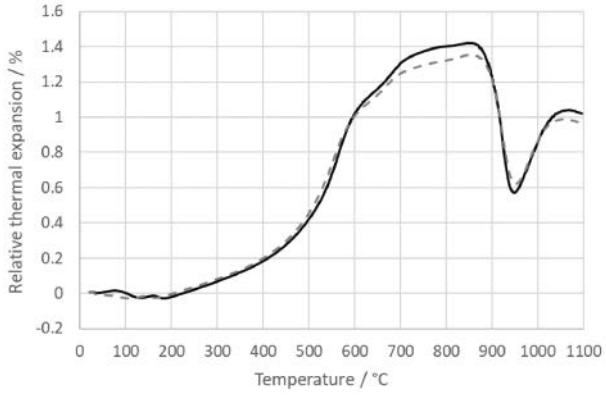


*Fig. 2* *The curves of relative thermal expansion for a thin sample (dashed line) and a thick sample (solid line)*
*2. ábra* *A relatív hőtágulás görbéi egy vékony minta (szaggatott vonal) és egy vastag minta (folytonos vonal) esetén*

Results of TDA are shown in *Fig. 2*, in which TDA curves for the thin sample (cross-section 4×4 mm²) and the thick sample (cross-section 8×8 mm²) are compared. Common dilatometers can measure samples with a cross-section of 8×8 mm², which in our case is the cross-section of the sample for D-TMA. If a thinner sample (4×4 mm²) is used, TDA results can differ to a small extent, but not more than 0.1%, and no shift between the curves is observed (*Fig. 2*). The ratio of Young's moduli is

$$\frac{E_{TDA\ of\ thin\ sample}}{E_{TDA\ of\ thick\ sample}} = \frac{1+0.014}{1+0.013} = 1.001\,. \qquad (6)$$

This result implies that TDA of the samples with different cross-sections does not give remarkable difference between Young's moduli.

*Fig. 3* shows temperature development of Young's modulus calculated from Eq. (4b), using TG results for the powder sample and the compact sample. The maximum difference between them is ~0.3 GPa in the region of the calcite decomposition, which represents 10%. The shown thermal development of Young's modulus is typical for firing the clays [4].

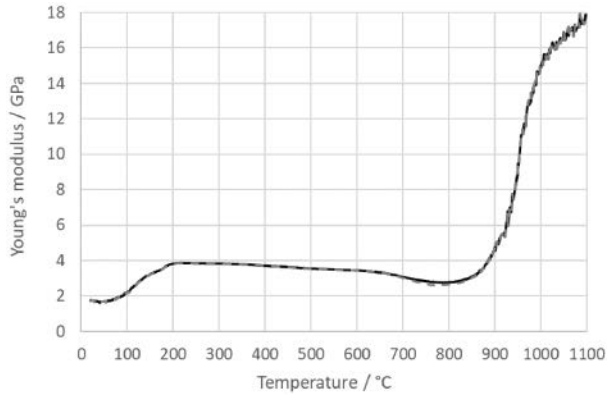


*Fig. 3* *The curves of Young's modulus when TG of the small powder sample was used (dashed line) and when TG of the compact sample was used (solid line) The difference between Young's moduli computed using the powder sample versus the compact sample in TG is driven by the processes that change the structure of some components of clay during heating.*
*3. ábra* *A Young-modulus görbéi, a kis porminta TG-adatai alapján (szaggatott vonal), illetve a tömör minta TG-adatai alapján (folytonos vonal) A Young-modulus értékeinek különbségét, amely a por és a tömör minta TG-adatai alapján számított értékek között jelentkezik, azok a folyamatok okozzák, amelyek a hevítés során megváltoztatják az agyag egyes komponenseinek szerkezetét.*

## 4. Conclusions

Natural illitic clay from Füzérradvány (Hungary) was mixed with powder calcite (22 wt.%), distilled water, and 3% solution of polyvinyl alcohol to obtain a plastic mass, from which prismatic samples were pressed. To determine the temperature dependence of Young's modulus, TG, TDA, and D-TMA have to be performed using three analyzers. The aim of this article was to show the influence of using different sample sizes and forms in TDA and TG on Young's modulus. The influence of the size of a TDA sample, which must be made from a compact material, was negligible. Contrary to the TDA sample, the form (solid or power) of the TG sample had a significant effect. If the small powder sample was used for TG, and its results were substituted into formula for Young's modulus, the relative error up to 10% can arise in the temperature region, where the change of some component is realized, e.g. decomposition of calcite in the described example.

In this study we also showed the importance of using compact samples with the same cross-section for TG, TDA, and IET in order to obtain correct values of Young's modulus during thermal treatment of the illitic clay.

## Acknowledgement

This work was supported by the grant of the Constantine the Philosopher University in Nitra UGA VII/9/2024 and Hungarian grant KIM 2024/0001768.

### References

[1] Norton, F. H. (1970) Fine Ceramics – Technology and Application. *McGraw-Hill Book Co.*, New York, 507 p.

[2] Hanykýř, V., Kutzendörfer, J. (2008) Technology of Ceramics. *Silikátový svaz*, Praha, 397 p. (in Czech)

[3] Kashtaljan, J. A. (1970) Elastic Characteristics of Materials at High Temperatures. Naukova Dumka, Kiev (in Russian)

[4] Húlan, T., Kaljuvee, T., Štubňa, I., Trník, A. (2016) Investigation of elastic and inelastic properties of Estonian clay from a locality in Kunda during thermal treatment. *Journal of Thermal Analysis and Calorimetry*. Vol. 124, No. 3, pp. 1153–1159, https://doi.org/10.1007/s10973-016-5280-6

[5] Štubňa, I., Vozár, L. (2005) The influence of the sample size on low-temperature processes in green electroceramics. *Industrial Ceramics*. Vol. 25, No. 2, pp. 110-112

[6] Štubňa, I., Trník, A., Podoba, R., Ondruška J., Vozár, L. (2014) The influence of thermal expansion and mass loss on the Young's modulus of ceramics during firing. *International Journal of Thermophysics*. Vol. 35, No. 9, pp. 1879-1887, https://doi.org/10.1007/s10765-012-1366-y

[7] Sokolář, R., Vodová, L., Grygarová, S., Štubňa, I., Šín, P. (2012) Mechanical properties of ceramic bodies based on calcite waste. *Ceramics International*. Vol. 38, No. 8, pp. 6607–6612 https://doi.org/10.1016/j.ceramint.2012.05.046

[8] Rath, J., et al. (1988) Fine Ceramics – Measurement Methods and Testing. *SNTL, Alfa*, Praha, Bratislava, 388 p. (in Czech)

[9] Štubňa, I., Trník, A., Vozár, L. (2011) Determination of Young's modulus of ceramics from flexural vibration at elevated temperatures. *Acta Acustica united with Acustica*. Vol. 97, No. 1, pp. 1–7, https://doi.org/10.3813/AAA.918380

[10] ASTM C1259-21 (2021) Standard test method for dynamic Young's modulus, shear modulus, and Poisson's ratio for advanced ceramics by impulse excitation of vibration. *ASTM International*, West Conshohocken, 18 p., https://doi.org/10.1520/C1259-21

[11] ASTM E1875-20a (2021) Standard test method for dynamic Young's modulus, shear modulus, and Poisson's ratio by sonic resonance. *ASTM International*, West Conshohocken, 10 p. https://doi.org/10.1520/E1875-20A

[12] Schreiber, E., Anderson, O., Soga, N. (1973) Elastic Constants and Their Measurement. *McGraw-Hill Book Co.*, New York, 196 p.

[13] Podoba, R., Trník, A., Podobník, Ľ. (2012) Upgrading of TGA/DTA analyzer Derivatograph. *Építőanyag*. Vol. 64, No. 1–2, pp. 28–29

[14] Štubňa, I., Húlan, T., Trník, A., Vozár, L. (2018) Uncertainty in the determination of Young's modulus of ceramics using the impulse excitation technique at elevated temperature. *Acta Acustica united with Acustica*. Vol. 104, No. 2, pp. 269–276, https://doi.org/10.3813/AAA.919169

Ref.:
**Kovács**, Tibor – **Štubňa**, Igor – **Trník**, Anton – **Vozár**, Libor: *Thermogravimetry and thermodilatometry as auxiliary analyses for dynamical thermomechanical analysis of clays*
Építőanyag – Journal of Silicate Based and Composite Materials, Vol. 77, No. 1 (2025), 15–18 p.
https://doi.org/10.14382/epitoanyag-jsbcm.2025.3

# Influence of black liquor on concrete performance: a sustainable approach

**Nasser A. M. BARAKAT** ▪ Chemical Engineering Department, Minia University, Minia, Egypt ▪ nasbarakat@mu.edu.eg
**Mamdouh M. NASSAR** ▪ Chemical Engineering Department, Minia University, Minia, Egypt
**Taha E. FARRAG** ▪ Chemical Engineering Department, Port Said University, Port Said, Egypt
**Hamdy A. A. MOHAMED** ▪ Qena Paper Company, Qena, Egypt
**Mohamed S. MAHMOUD** ▪ University of Technology and Applied Sciences-Suhar, College of engineering and technology, Department of Engineering, Sultanate of Oman ▪ mohamed.mohamed@utas.edu.om

Érkezett: 2025. 02. 17. ▪ Received: 17. 02. 2025. ▪ https://doi.org/10.14382/epitoanyag-jsbcm.2025.4

**Abstract**

The integration of industrial by-products into concrete mixtures has gained significant attention as a sustainable approach to improving material performance while reducing environmental impact. This study investigates the effects of black liquor (BL), a lignin-rich by-product of the paper industry, as a novel admixture in concrete. Concrete samples with varying BL concentrations (0–4 wt.%) were prepared and evaluated for mechanical strength, workability, density, porosity, and microstructural modifications. The results indicate that the incorporation of 2 wt.% BL optimally enhances concrete properties, yielding a 25% increase in compressive strength (from 40 MPa to 50 MPa) at 28 days. Furthermore, splitting tensile and flexural tensile strengths peaked at 3.6 MPa and 15 MPa, respectively, at this concentration. Workability improved significantly, as evidenced by a 200% increase in slump value compared to BL-free concrete. Additionally, bulk density reached its maximum at 2.28 kg/L, while apparent porosity exhibited a notable decline to 9%, indicating matrix densification. Scanning electron microscopy (SEM) confirmed the refinement of pore structure and enhanced cementitious bonding at 2 wt.% BL. However, excessive BL content (≥3 wt.%) led to reduced performance due to increased porosity and disruption of cement hydration. These findings highlight the potential of black liquor as an effective and sustainable concrete admixture, offering enhanced mechanical properties and improved durability while promoting industrial waste reutilization.

Keywords: Black liquor; Sustainable concrete; Mechanical properties; Microstructure; Porosity reduction
Kulcsszavak: fekete lúg, fenntartható beton, mechanikai tulajdonságok, mikrostruktúra, porozitáscsökkenés

## 1. Introduction

Concrete is the most widely used construction material globally due to its versatility, durability, and cost-effectiveness. However, the environmental impact of concrete production, primarily attributed to the carbon emissions associated with cement manufacturing, has driven researchers to explore sustainable alternatives and admixtures. One such approach is the incorporation of industrial by-products to improve concrete properties while minimizing environmental harm. Among these, black liquor (BL), a by-product of the paper industry, has gained attention for its potential as a sustainable admixture.

The global production of cement, a critical component of concrete, accounts for approximately 8% of total carbon dioxide emissions annually [1, 2]. Efforts to mitigate this environmental footprint have focused on reducing clinker content, utilizing supplementary cementitious materials (SCMs), and incorporating waste products. Black liquor, which is rich in lignin and organic compounds, presents an opportunity to address these challenges [3]. It is generated in large quantities during the kraft pulping process, with global production exceeding 60 million tons per year [4]. Without proper utilization, black liquor poses significant disposal and environmental issues, including water pollution and toxicity [5].

The chemical composition of black liquor makes it a promising candidate for concrete admixture. It contains lignin, hemicellulose, and other organic compounds, which exhibit pozzolanic activity and can influence the hydration

**Nasser A. M. BARAKAT**
Nasser A. M. Barakat is a renowned Professor of Chemical Engineering at Minia University, Egypt. He earned his Ph.D. in Chemometrics from Hunan University, China, and has held academic positions at Chonbuk National University in South Korea. His research focuses on advanced materials, including electrospun nanofibers, energy applications, and water treatment technologies. Professor Barakat has published extensively, with significant contributions to the fields of nanotechnology and environmental engineering. His work has garnered numerous citations and awards, reflecting his impact and leadership in chemical engineering

**Mamdouh M. NASSAR**
Professor Emeritus of Chemical Engineering at Minia University, Egypt. He earned his Ph.D. in Chemical Engineering from the Technical University of Norway in 1975, following a Diploma in Pulping Technology and an M.Sc. from Alexandria University. With a career span of over five decades, Professor Nassar has held various academic and administrative positions, including Vice Dean of Student Affairs and Head of the Chemical Engineering Department at Minia University. His research focuses on mass transfer operations, adsorption engineering, and effluent treatment, contributing significantly to the field through numerous publications and collaborations

**Taha E. FARRAG**
Is a distinguished Professor of Chemical Engineering at Port Said University, Egypt. He currently serves as the Dean of the Faculty of Engineering. With a robust academic background and extensive research experience, Professor Farrag specializes in transport phenomena and the application of mass transfer techniques for wastewater treatment. His scholarly contributions include numerous publications on topics such as adsorption processes and water desalination. Professor Farrag's work has significantly advanced the field of chemical engineering, earning him recognition and citations in various academic circles

**Hamdy A. A. MOHAMED**
Ph.D. student at Department of Chemical Engineering, Minia University, El Minia, Egypt. Senior head of operation section at Qena Paper industry, Qena, Egypt. Member, Egyptian Society of Engineers. His expertise in industrial operations and commitment to excellence have played a crucial role in maintaining the high standards of Quena Paper Factory, one of the leading manufacturers of printing and writing paper in the region

**Mohamed S. MAHMOUD**
Associate Professor at the Chemical Engineering Department of Minia University, Egypt. He also serves as an Assistant Professor at the University of Technology and Applied Sciences (UTAS) in Suhar, Oman, where he is the Head of the Scientific Research Department. With a strong academic background and extensive research experience, Dr. Mahmoud specializes in areas such as high temperature reactions, wastewater treatment, nanotechnology, green hydrogen production and carbon. His contributions to the field are reflected in numerous publications and his leadership roles in both academic institutions

process of cement [6, 7]. Previous studies have demonstrated that lignin-based materials can enhance workability, reduce water demand, and improve the durability of concrete [8, 9]. Additionally, black liquor's ability to act as a retarder has been reported to extend setting times, providing greater flexibility during construction [10].

The incorporation of black liquor in concrete has been shown to improve mechanical properties under optimal conditions. For example, Kemal *et al* [11] observed that organic compounds in black liquor interact with calcium hydroxide (CH) to form additional calcium silicate hydrate (C-S-H) gels, which densify the matrix and enhance strength. Hassan *et al* [12] reported that admixtures derived from lignin improve the compressive strength and reduce porosity, which are critical for durability. However, excessive black liquor content can lead to increased porosity and reduced strength due to the disruption of hydration and bonding [13].

Utilizing black liquor in concrete not only enhances its properties but also aligns with the principles of sustainable development. By repurposing a waste product, this approach reduces the reliance on synthetic admixtures and minimizes industrial waste [14]. Additionally, it supports circular economy practices in the paper industry by creating value from by-products [15]. Previous research has highlighted the potential of black liquor to significantly reduce the carbon footprint of construction materials while addressing waste management issues [16, 17].

While several studies have explored the use of lignin and its derivatives in concrete, the specific effects of black liquor on mechanical properties, microstructure, and setting times remain underexplored. This study aims to fill this gap by systematically investigating the impact of varying black liquor contents (0–4 wt.%) on concrete properties. By integrating experimental findings with microstructural insights, this study seeks to establish black liquor as a viable and sustainable admixture for concrete production. The results have implications for both the construction and paper industries, offering a pathway toward more sustainable and high-performance.

## 2. Materials and methods

### 2.1 Materials

The primary materials used in this study include Ordinary Portland Cement (OPC), natural sand, crushed gravel, and black liquor (BL).

- Cement: OPC (Grade 42.5) was used as the binder, conforming to ASTM C150 standards.
- Sand: Natural river sand with a fineness modulus of 2.6 was used as fine aggregate.
- Gravel: Crushed gravel with a maximum size of 20 mm was employed as coarse aggregate.
- Black Liquor: BL was obtained from Qena Paper Industry Company, Quse, Egypt. Its chemical composition includes lignin, hemicellulose, and inorganic compounds, contributing to its pozzolanic activity.
- Water: Potable water was used for mixing and curing.

### 2.2 Sample preparation

Concrete mixes were prepared with varying BL contents of 0%, 1%, 2%, 3%, and 4% by weight of cement. Three different concrete samples (S1, S2, S3) were formulated based on *Table 1*:

| Sample code | Ingredients | | | |
|---|---|---|---|---|
| | Cement (kg/m³) | Gravel (kg/m³) | Sand (kg/m³) | Water/cement ratio |
| **S1** | 360 | 1410 | 705 | 0.47 |
| **S2** | 380 | 1385 | 692 | 0.47 |
| **S3** | 400 | 1360 | 680 | 0.47 |

*Table 1 Prepared samples composition*
*1. táblázat Az előkészített minták összetétele*

The mixing process followed ASTM C192, involving the sequential addition of aggregates, cement, water, and BL to ensure uniform distribution.

### 2.3 Testing methods

#### 2.3.1 Mechanical properties

- *Compressive strength:* Tested according to ASTM C39 using a 2000 kN capacity compression testing machine. Specimens were cured for 1, 3, 7, 14, 28, and 90 days, with results recorded as the average of three specimens.
- *Splitting tensile strength:* Measured using ASTM C496 standards on cylindrical specimens. The load was applied diametrically using a 1000 kN capacity testing machine.
- *Flexural strength:* Conducted on prismatic beams following ASTM C78 standards. A three-point loading system was applied.

#### 2.3.2 Durability and physical properties

- *Bulk density:* Determined by dividing the dry weight of specimens by their volume. Measured for each curing period.
- *Apparent porosity:* Evaluated using Archimedes' principle by measuring the saturated and dry weights of the specimens.
- *Initial and final setting times:* Assessed using Vicat apparatus per ASTM C191. BL's impact on hydration dynamics was observed for each mix.

#### 2.3.3 Workability (Slump Test)

Slump value was measured using the ASTM C143 standard slump cone test. The effect of BL content (0%, 1%, 2%, 3%, 4%) on workability was evaluated by determining the slump value for each mix. Measurements were recorded to the nearest millimeter, highlighting changes in flowability with varying BL concentrations.

The slump test was conducted following ASTM C143 standards. The procedure is as follows:

1. *Equipment:* A standard slump cone (300 mm in height, 200 mm bottom diameter, 100 mm top diameter), a tamping rod, and a flat base plate were used.

2. *Preparation:* The slump cone was placed on the flat base plate, and the internal surface was lightly oiled to prevent sticking.
3. *Filling:* The cone was filled with concrete in three layers, each approximately one-third of the cone's height.
4. *Compaction*: Each layer was compacted using 25 strokes of the tamping rod, uniformly distributed across the surface.
5. *Leveling:* After the third layer, the excess concrete was struck off to level the surface with the top of the cone.
6. *Lifting the Cone:* The cone was lifted vertically and steadily within 5–10 seconds to avoid lateral displacement of the concrete.
7. *Measurement:* The slump value was determined by measuring the vertical displacement (difference in height) between the top of the slump cone and the highest point of the slumped concrete.

#### 2.3.3 Microstructural analysis

Scanning Electron Microscopy (SEM) images were captured using a JEOL JSM-6510LV microscope. Samples from 0% and 2% BL mixes were analyzed to evaluate the microstructural changes.

All tests were conducted under controlled laboratory conditions, with an ambient temperature of 25 ± 2°C and relative humidity of 50%. Each test was repeated three times to ensure reproducibility and accuracy. Data were statistically analyzed using ANOVA to determine the significance of the observed differences among the mixes. A significance level of 0.05 was considered for all analyses.

## 3. Results and discussion

*Fig. 1* shows the influence of black liquor content on the compression strength of the prepared concrete mixtures. As shown, in general, the addition of black liquor (BL) at different concentrations (0–4 wt.%) significantly affects the compressive strength of concrete samples (S1, S2, S3) over time (1, 3, 7, 14, and 28 days). Across all samples:

- The compressive strength increases with curing time, reaching its maximum at 28 days.
- Optimal black liquor content lies at 2 wt.%, where the compressive strength is at its peak. Beyond this concentration, the strength diminishes. Numerically, the determined compression strengths at 2 wt.% BL after 28 days aging time were 46, 46.8 and 48.8 MPa for S1, S2 and S3 samples, respectively.

Black liquor contains organic compounds and lignin, which may act as retarders or pozzolanic additives, influencing hydration, setting time, and strength development. The observed effects can be attributed to the pozzolanic activity. At optimal concentrations (2 wt.%), black liquor contributes to secondary hydration reactions, forming additional calcium silicate hydrates (C-S-H), which enhance strength. Studies confirm that lignin and other organic substances in black liquor react with calcium hydroxide to produce C-S-H gels [7]. The addition of black liquor improves the workability of concrete, potentially resulting in better compaction and reduced porosity. This is in line with research on admixtures derived from lignin-based substances [8]. Excessive black liquor (3–4 wt.%) likely introduces too much organic matter, which interferes with the cement hydration process, increases porosity, and weakens the concrete matrix [18].

### Comparison of Samples (S1, S2, S3)

- *S1 (Low cement content; Fig. 1A):* Shows lower compressive strength overall. The addition of black liquor is beneficial but limited by the lower cement content, reducing the extent of hydration and pozzolanic reactions.
- *S2 (Moderate cement content; Fig. 1B):* Exhibits higher strength compared to S1 due to increased cement content, which supports more extensive hydration and secondary reactions facilitated by black liquor.
- *S3 (High cement content; Fig. 1C)*: Achieves the highest compressive strength among the samples. The improved hydration and densified matrix due to the interaction of black liquor with the high cement content explain its performance.

The strength development over time aligns with the typical hydration process. For instance, at 1 day, hydration is minimal, and black liquor primarily acts as a plasticizer, slightly improving strength. By 7 and 14 days, secondary hydration becomes more pronounced, and black liquor's pozzolanic activity maximizes strength. At 28 days, the matrix becomes denser, and the strength stabilizes, highlighting the long-term effects of black liquor.

In conclusion, using black liquor at 2 wt.% offers a sustainable way to enhance concrete properties, leveraging waste materials while reducing cement usage. Incorporating black liquor reduces industrial waste and promotes eco-friendly construction practices. However, the performance is sensitive to the dosage of black liquor and the initial composition of the concrete mix.

*Fig. 2* shows the influence of aging time on the compression strength at the optimum black liquor content (2 wt.%). The data for sample S1 (as a model, the other two samples show similar behavior (data are not shown). As shown in the figure, the compressive strength increases significantly within the first 28 days, stabilizing thereafter with only a slight increase observed at 90 days: 43.5 and 46 MPa after 28 and 90 days, respectively. This pattern aligns with the general hydration process of cementitious materials, where the rate of hydration slows over time as the reaction nears completion.

The observed results can be attributed to the interplay between hydration, pozzolanic activity, and the role of black liquor. During the initial 28 days, the hydration of cement generates calcium silicate hydrates (C-S-H) and calcium hydroxide (CH), which are the primary contributors to strength development. Black liquor at 2 wt.% optimally enhances the formation of dense C-S-H gel, filling pores and reducing micro-cracks [6].

Black liquor introduces lignin and other organic compounds that act as secondary reactants. These compounds react with CH to form additional C-S-H gels, especially prominent in the first 28 days. This aligns with studies showing lignin-based materials' capability to improve strength through enhanced pozzolanic reactions [9]. Beyond 28 days, most CH is consumed, leading to a plateau in compressive strength.

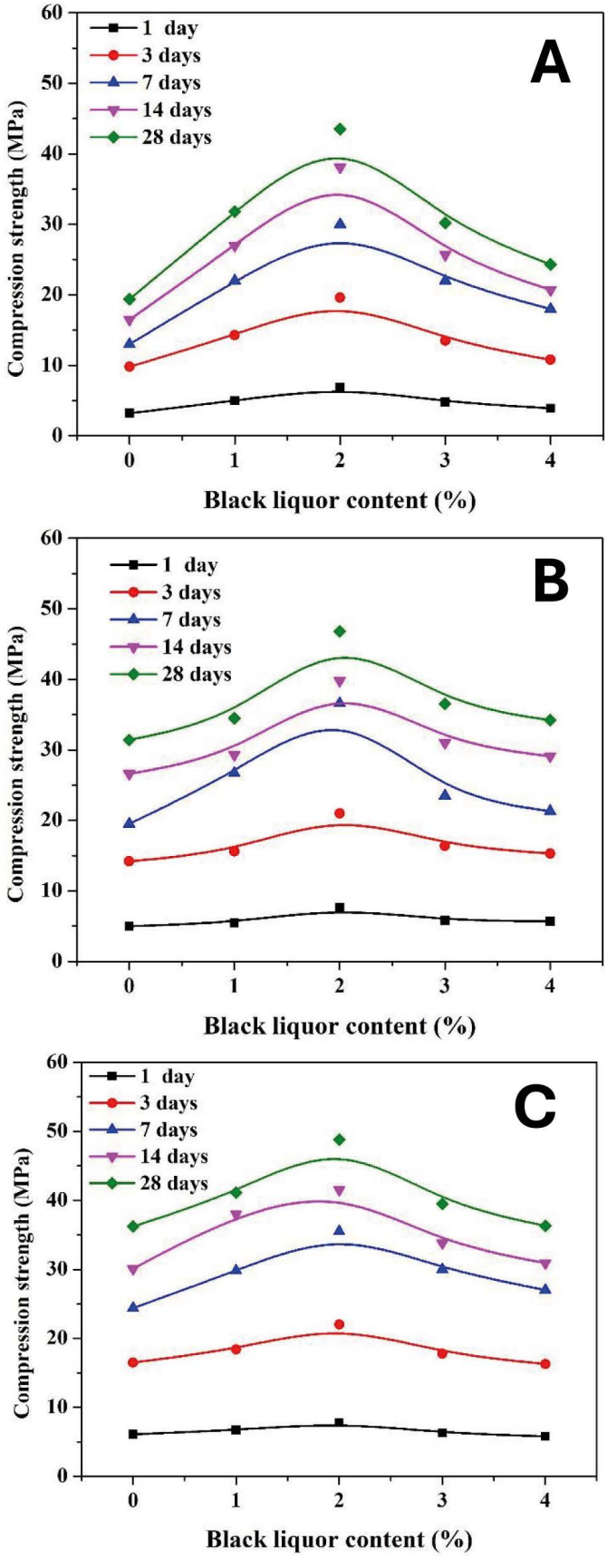


*Fig. 1 Effect of black liquor content on the compression strength of the prepared concrete samples: S1; (A), S2; (B) and S3; (C)*

*1. ábra A fekete lúg tartalom hatása az előállított betonminták nyomószilárdságára S1; (A), S2; (B) and S3; (C)*

The optimal black liquor content helps refine the microstructure by reducing porosity and enhancing particle packing, as confirmed by studies on similar lignin-based admixtures [18]. The slight strength gains between 28 and 90 days likely results from the continued slow hydration of unreacted clinker phases and secondary pozzolanic reactions.

In conventional concrete without black liquor, compressive strength typically exhibits a slower rate of gain, particularly beyond 28 days. The introduction of black liquor accelerates early strength gain while maintaining long-term performance. This improvement is consistent with studies emphasizing the role of organic admixtures in promoting early strength while ensuring sustainability [18].

The accelerated strength development within 28 days makes black liquor-enhanced concrete suitable for time-sensitive construction projects where early loading is required. Utilizing black liquor, a waste product from the paper industry, promotes eco-friendly practices by reducing waste and minimizing cement usage, thereby lowering the carbon footprint. The stability of compressive strength at 90 days indicates the material's durability and long-term reliability.

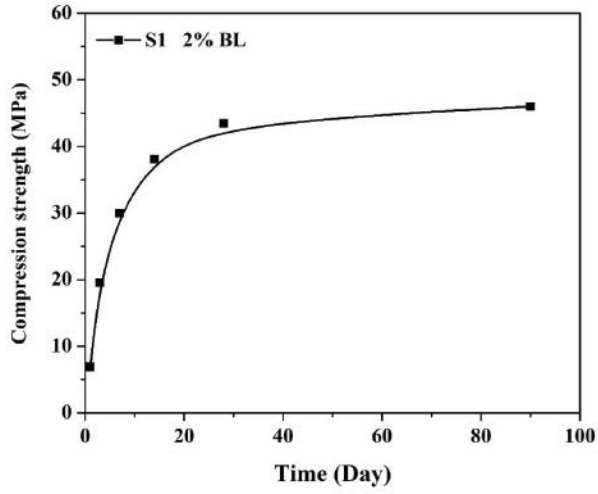


*Fig. 2 Effect of residence time on the compression strength of S1 containing 2 % black liquor*

*2. ábra A tartózkodási idő hatása az S1 minták nyomószilárdságára 2%-os fekete lúg tartalom mellett*

*Fig. 3A* shows the influence of black liquor content on the splitting tensile strength of the utilized three samples. As shown, the splitting tensile strength of the concrete samples (S1, S2, S3) exhibits a parabolic trend with varying black liquor (BL) content. A steady increase in tensile strength is observed with BL content up to 2 wt.%, followed by a gradual decline beyond this concentration. Sample S3 demonstrates the highest splitting tensile strength, followed by S2 and S1, in alignment with their respective cement contents. Numerically, the determined splitting tensile strengths for the three samples were 2.83, 3.24 and 3.52 MPa for S1, S2 and S3 samples, respectively.

The splitting tensile strength of concrete is influenced by its composition, microstructure, and the interaction of additives like black liquor with the cement matrix. As aforementioned,

black liquor's lignin and organic compounds contribute to pozzolanic reactions, consuming calcium hydroxide (CH) and forming additional calcium silicate hydrate (C-S-H) gels. These gels enhance the bond strength within the concrete, improving its tensile properties [19]. At 2 wt.% BL, the organic components likely improve workability and compaction, reducing voids and enhancing the tensile load-bearing capacity [18]. At higher BL concentrations (3–4 wt.%), excessive organic compounds disrupt the hydration process and increase porosity, leading to weaker tensile strength. This phenomenon aligns with previous findings on the detrimental effects of over-admixturing in concrete [20]. The inclusion of BL at 2 wt.% may result in improved aggregate-cement paste adhesion, critical for tensile strength. Improved adhesion reduces crack propagation under tensile loads, explaining the observed peak at 2 wt.% [6].

Lowest splitting tensile strength was observed with the lowest cement content sample (S1) due to limited cement content and reduced hydration product formation. The addition of BL provides some improvement but is constrained by the overall composition. For S2 sample, the sample exhibits better tensile strength than S1, reflecting the synergistic effect of BL and higher cement content. BL optimally interacts with the higher volume of cementitious materials to enhance tensile properties. However, S3 achieves the highest tensile strength, benefiting from the ample cement content and the optimized interaction with BL. The matrix is denser, with fewer micro-cracks, leading to superior performance.

Adding black liquor up to 2 wt.% can enhance splitting tensile strength, making concrete more suitable for applications requiring tensile stress resistance, such as pavements and slabs. Black liquor, being a by-product of the paper industry, offers a sustainable and cost-effective alternative to synthetic additives, contributing to waste management and reduced cement consumption. Careful control of BL dosage is necessary to avoid the negative impacts of excess organic material on concrete's tensile properties.

*Fig. 3B* displays the effect of the black liquor content on the flexural tensile strength of the three concrete samples (S1, S2, S3). As shown, the flexural tensile strength follows a parabolic trend similar to that observed in compressive and splitting tensile strength. The strength improves with increasing black liquor (BL) content up to 2 wt.%, where it reaches a maximum, and declines beyond this concentration. Sample S3 exhibits the highest flexural tensile strength due to its higher cement content, followed by S2 and S1, consistent with the trends observed for other mechanical properties. Numerically, the determined flexural tensile strengths were 13.3, 14.5 and 15.2 MPa for S1, S2 and S3 samples, respectively.

Flexural tensile strength is governed by the concrete matrix's resistance to bending stresses, which depends on its composition, microstructure, and the distribution of stresses across the section. At 2 wt.% BL, the organic compounds in black liquor act as pozzolanic additives, promoting the formation of additional C-S-H gels. These gels fill voids and enhance the bond between aggregates and the cement paste, resulting in higher flexural strength [3, 7]. The improved microstructure at this concentration minimizes crack initiation and propagation under bending stresses, leading to higher flexural performance [6].

At higher BL contents (3–4 wt.%), excess lignin and organic compounds increase porosity and reduce the effectiveness of the cement hydration process. This weakens the matrix and reduces its ability to resist bending stresses [18]. The observed flexural tensile strength trends are closely linked to compressive and splitting tensile strength. The peak performance at 2 wt.% BL is consistent across all strength tests, confirming this concentration as optimal for enhancing the concrete's mechanical properties. The decline beyond 2 wt.% BL highlights the diminishing returns of excess organic material in all strength parameters, underscoring the importance of controlled admixture dosages. Sample hierarchy (S3 > S2 > S1) trend reflects the critical role of cement content in enabling the matrix to utilize the beneficial effects of BL effectively. The same hierarchy was observed for compressive and splitting tensile strengths, emphasizing the interplay between composition and admixture performance.

Flexural tensile strength is particularly sensitive to microstructural properties such as aggregate – cement paste bonding and porosity. The role of BL in reducing voids and improving cohesion between matrix components at 2 wt.% contributes significantly to the observed improvements. The use of BL at 2 wt.% improves the flexural capacity of concrete, making it suitable for applications subject to bending stresses, such as beams, slabs, and pavements. The simultaneous enhancement of compressive, splitting tensile, and flexural tensile strengths highlights the versatility of BL as a sustainable additive. Utilizing BL, a waste by-product of the paper industry, aligns with eco-friendly construction practices by reducing cement consumption and waste disposal issues.

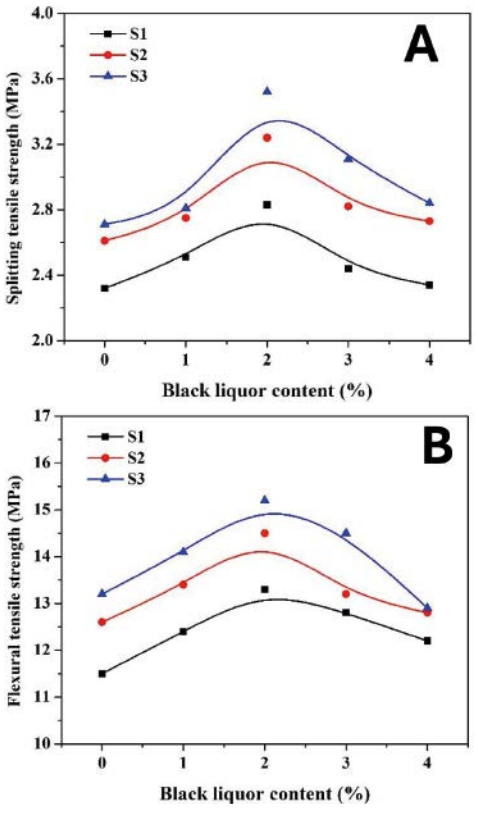


*Fig. 3 Effect of black liquor content on the splitting; (A) and flexural; (B) tensile strength of the prepared concrete samples*

*3. ábra A fekete lúg tartalom hatása az előállított betonminták hasító- (A) és hajlító- (B) húzószilárdságára*

*Fig. 4A* represents the effect of the BL content on the initial setting time of the prepared concrete samples. As shown, the initial setting time of the concrete samples (S1, S2, S3) increases with the addition of black liquor (BL) content:

- At 0 wt.% BL, the initial setting time is approximately 80 minutes for all samples.
- At 2 wt.% BL (optimal content for strength properties), the initial setting time increases to about 140 minutes.
- At 4 wt.% BL, the setting time reaches around 190 minutes, indicating a significant delay.

This trend suggests that black liquor acts as a retarding admixture, slowing down the hydration process and extending the time before the concrete begins to set.

Black liquor contains organic compounds like lignin and sugars, which are known to adsorb onto cement particles. This adsorption creates a barrier that delays the hydration reaction of cement, leading to an increase in setting time [6, 21].

At lower BL concentrations (1–2 wt.%), the retarding effect is moderate, allowing sufficient hydration to develop strength while extending workability. At higher concentrations (3–4 wt.%), the abundance of organic molecules excessively hinders hydration, causing prolonged delays in setting time.

The increase in setting time at 2 wt.% BL aligns with the enhanced mechanical properties (compressive, splitting tensile, and flexural tensile strengths). The delayed setting provides additional time for particle rearrangement and densification of the concrete matrix, contributing to improved strength development. This balance between delayed setting and optimal hydration underscores the beneficial effects of controlled BL addition. At 3–4 wt.% BL, the extended setting time correlates with reduced strength properties. Excessive retardation limits the formation of hydration products within a reasonable timeframe, resulting in weaker concrete [18].

S1 exhibits slightly higher setting times compared to S2 and S3 across all BL concentrations, likely due to its lower cement content and reduced hydration rate. However, S2 and S3 samples show comparable setting times, with S3 demonstrating marginally shorter times at higher BL contents. This reflects the influence of higher cement content in promoting faster hydration despite the presence of BL.

The increased setting time with BL addition enhances workability, making the concrete easier to handle and place, particularly in complex construction projects. The extended setting time at higher BL concentrations could delay construction processes, requiring adjustments in scheduling. By incorporating BL as a retarding admixture, the reliance on synthetic retarders can be reduced, promoting eco-friendly and cost-effective practices.

*Fig. 4B* displays the influence of the BL content on the final setting time of the prepared concrete samples. As shown, the final setting time of concrete samples (S1, S2, S3) increases linearly with the addition of black liquor (BL) content:

- At 0 wt.% BL, the final setting time is approximately 150 minutes for all samples.
- At 2 wt.% BL (optimal content for strength properties), the final setting time increases to around 270 minutes.
- At 4 wt.% BL, the setting time reaches approximately 400 minutes, indicating a significant delay.

This result parallels the trend observed for the initial setting time, confirming black liquor's role as a retarding admixture. Similar to the initial setting time, the presence of lignin and other organic substances in black liquor delays hydration by forming a temporary barrier around cement particles. This results in a prolonged final setting time. At low BL concentrations (1–2 wt.%), the retarding effect is controlled, ensuring sufficient hydration while extending workability. Higher BL concentrations (3–4 wt.%) exacerbate the delay, slowing hydration excessively and prolonging the final setting process.

The relationship between initial and final setting times remains consistent across BL concentrations. At 0 wt.% BL, the time gap between initial and final setting is approximately 70 minutes (80–150 minutes). At 2 wt.% BL, the gap increases to 130 minutes (140–270 minutes), reflecting a greater overall retardation effect. At 4 wt.% BL, the gap further widens to 210 minutes (190–400 minutes). This proportional increase suggests that black liquor uniformly influences both stages of the setting process, delaying the onset and progression of hydration reactions.

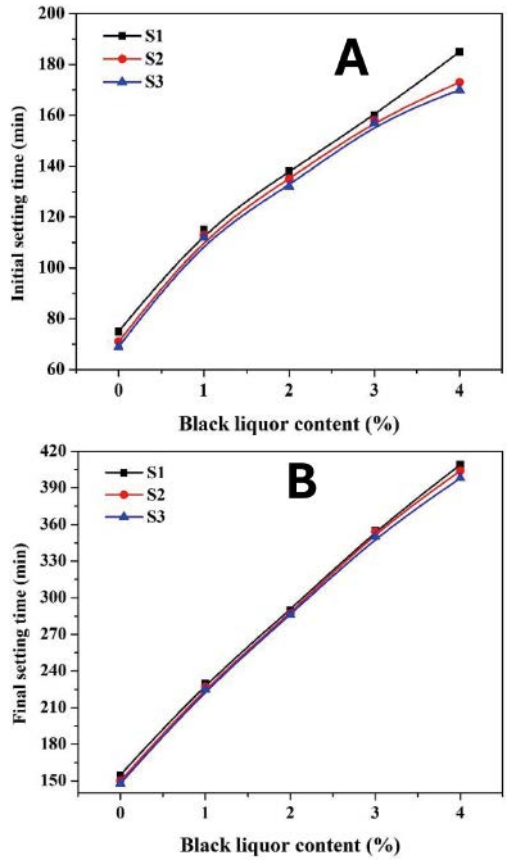


*Fig. 4 Effect of black liquor content on the initial and final setting times of the prepared concrete samples.*
*4. ábra A fekete lúg tartalom hatása az előállított betonminták kötési idejének kezdetére és a teljes kötési időre*

At 2 wt.% BL, the extended final setting time allows for better compaction and hydration, contributing to enhanced mechanical properties, as observed in compressive, splitting tensile, and flexural tensile strengths. The balance between delayed setting and optimized hydration underscores the

suitability of this concentration for practical applications. Excessive delay in final setting at these concentrations correlates with reduced mechanical properties. The extended hydration period limits the timely formation of hydration products, weakening the overall matrix. The extended setting times improve workability, allowing for better handling and placement of concrete in complex structures. Excessive delays at higher BL contents may disrupt construction schedules, necessitating careful control of dosage. Black liquor provides an eco-friendly alternative to synthetic retarders, reducing environmental impact while enhancing concrete properties.

*Fig. 5* demonstrates the impact of the BL content on the bulk density of the prepared concrete samples. As shown, the bulk density of the concrete samples increases with black liquor (BL) content up to 2 wt.%, followed by a slight decline at higher concentrations. Numerically, at 0 wt.% BL, the bulk density is approximately 2.16 kg/l at 1 day and gradually increases over time. At 2 wt.% BL, the bulk density peaks around 2.25–2.28 kg/l (depending on curing time), corresponding to the optimal BL content observed for mechanical properties. Beyond 2 wt.% BL, the bulk density decreases slightly, stabilizing at approximately 2.22–2.23 kg/l at 4 wt.% BL for long curing times (90 days).

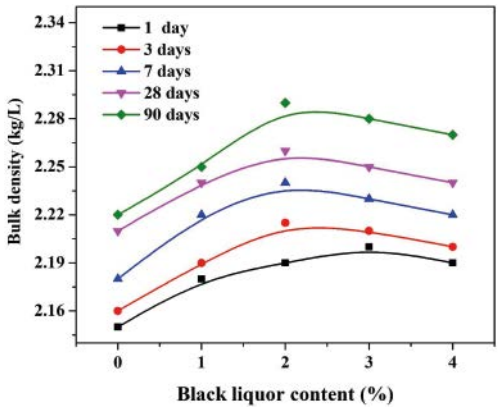


*Fig. 5 Effect of black liquor content on the bulk density of the concrete of S1 sample*
*5. ábra A fekete lúg tartalom hatása az S1 betonminta testsűrűségére*

The introduction of black liquor improves compaction and reduces voids in the concrete matrix up to 2 wt.%, resulting in higher bulk density. This is supported by the enhanced particle packing and matrix densification due to secondary pozzolanic reactions that generate additional C-S-H gels. At higher BL contents (3–4 wt.%), the organic components increase porosity by disrupting the hydration process and forming weak zones within the matrix. This reduces the bulk density despite prolonged curing times. At the early stage (1 to 7 days), The bulk density increases rapidly during the first week, reflecting the hydration of cement and the contribution of black liquor to early matrix densification. For instance, at 2 wt.% BL, the bulk density increases from 2.18 kg/l (1 day) to approximately 2.25 kg/l (7 days). Over time, the hydration slows, and the bulk density stabilizes. At 90 days, the bulk density for samples with 2 wt.% BL reaches its peak (~2.28 kg/l), indicating a fully developed matrix.

The peak bulk density at 2 wt.% BL aligns with the highest values observed for compressive, splitting tensile, and flexural tensile strengths. This highlights the role of dense matrix formation in enhancing mechanical performance. The improved bulk density at this concentration reduces porosity, ensuring better load distribution and crack resistance. The decrease in bulk density beyond 2 wt.% correlates with reduced mechanical strengths, emphasizing the detrimental effect of excessive organic content on matrix integrity.

Increased bulk density up to 2 wt.% BL indicates improved workability and durability, making the material suitable for applications requiring dense and durable concrete. The decline in bulk density at higher BL concentrations suggests limitations for structural applications where strength and compactness are critical.

*Fig. 6* displays the influence of BL content on the apparent porosity of the prepared concrete. As shown, the apparent porosity of concrete samples decreases significantly with the addition of black liquor (BL) content up to 2 wt.% and increases slightly beyond this concentration. At 0 wt.% BL, the porosity is highest, approximately 16% at 1 day and reduces to about 13% at 90 days due to hydration and matrix densification. At 2 wt.% BL, the porosity reaches its lowest point, approximately 10.5% at 1 day and 9% at 90 days, reflecting optimal densification. Beyond 2 wt.% BL, the porosity increases slightly, stabilizing around 11% at 90 days for 4 wt.% BL. This trend confirms black liquor's ability to reduce porosity by enhancing matrix densification and particle packing up to an optimal concentration.

The organic compounds in black liquor act as a plasticizer, improving the workability of the concrete and allowing better compaction. This results in reduced voids and a denser microstructure at optimal concentrations [22, 6]. The secondary pozzolanic reactions triggered by black liquor produce additional C-S-H gels, filling the pores and further reducing porosity. At higher BL concentrations (3–4 wt.%), excessive organic material disrupts hydration and may lead to poor bonding within the matrix. This creates microvoids and weak zones, increasing porosity.

The decrease in apparent porosity at 2 wt.% BL aligns with the peak in bulk density (~2.28 kg/l). This correlation highlights the role of reduced porosity in improving density and overall compactness. At higher BL contents, the increase in porosity correlates with the slight decline in bulk density, confirming the inverse relationship between these properties. The lowest porosity at 2 wt.% BL contributes to the highest compressive, splitting tensile, and flexural tensile strengths. The denser matrix reduces crack initiation and propagation, resulting in superior mechanical performance. At higher BL concentrations, increased porosity weakens the matrix, leading to reduced mechanical properties.

Apparent porosity decreases rapidly during the first week due to early hydration and the formation of C-S-H gels. For example, at 2 wt.% BL, porosity decreases from 10.5% (1 day) to 9.5% (7 days). Long-term curing further reduces porosity, particularly at optimal BL content. At 90 days, porosity for 2 wt.% BL reaches its minimum (~9%), reflecting a fully developed matrix.

Reduced porosity at 2 wt.% BL improves durability by minimizing water ingress and resistance to environmental degradation. The results emphasize the importance of using BL at its optimal concentration (2 wt.%) to balance porosity reduction with mechanical performance.

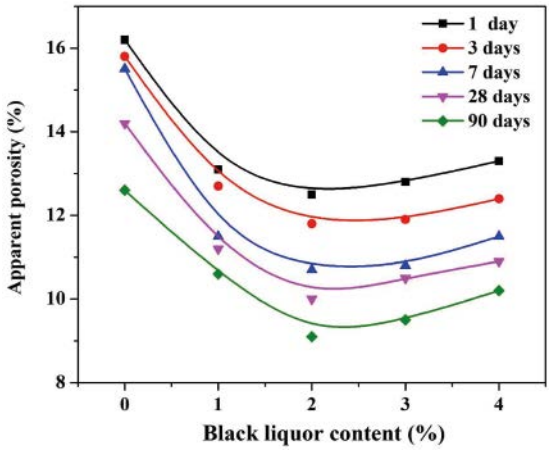


*Fig. 6 Effect of black liquor content on the apparent porosity of S1 sample*
*6. ábra A fekete lúg tartalom hatása az S1 minta látszólagos porozitására*

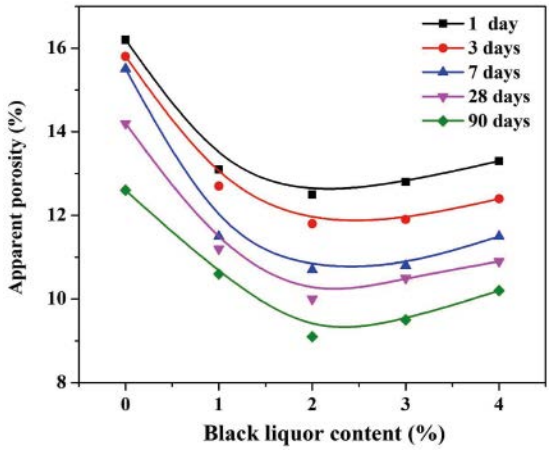


*Fig. 7 Effect of black liquor content on the slump value of the prepared concrete samples*
*7. ábra A fekete lúg tartalom hatása az előállított betonminták roskadási értékére*

The slump value of concrete samples (S1, S2, S3) (shown in *Fig. 7*) increases with the addition of black liquor (BL) content across all tested mixes. Typically, at 0 wt.% BL, the slump value is approximately 25 mm, indicating relatively low workability. At 2 wt.% BL, the slump value increases to around 100 mm, reflecting a significant improvement in workability. At 4 wt.% BL, the slump value reaches its maximum, approximately 200 mm for S1, with similarly high values observed for S2 and S3. This trend demonstrates that black liquor effectively enhances the workability of concrete by increasing its slump value.

Black liquor contains lignin and other organic compounds that act as natural plasticizers, reducing the internal friction between particles and allowing the concrete to flow more freely [3]. These compounds also improve the dispersion of cement particles, reducing water demand and enhancing fluidity [23]. Black liquor's organic content enhances the water-retaining capacity of the mix, which contributes to higher slump values [24]. The improved lubrication within the mix reduces resistance to flow, increasing workability without compromising the water-to-cement ratio.

The first sample (S1) exhibits the highest slump values across all BL concentrations, likely due to its lower cement content, which reduces the viscosity of the mix. However, both S2 and S3 samples show slightly lower slump values compared to S1, consistent with their higher cement content, which increases the paste viscosity and slightly restricts flow.

The increased workability at higher BL concentrations is consistent with the observed extension in setting times. The retarding effect of BL allows for greater slump values, improving handling and placement in construction. While higher slump values improve workability, excessive BL content (3–4 wt.%) can compromise mechanical properties due to increased porosity and disrupted hydration dynamics, as previously discussed. The enhanced workability provided by BL addition makes the concrete easier to handle, place, and compact, particularly in complex or heavily reinforced structures. While 4 wt.% BL maximizes the slump value, 2 wt.% BL provides a balanced improvement in workability and mechanical properties, making it the optimal concentration for practical applications.

The SEM images (*Fig. 8*) of the S2 sample with 0% BL and 2% BL provide direct evidence of the microstructural changes induced by the addition of black liquor. For the BL-free sample (*Fig. 8B*), the microstructure shows larger voids and less cohesive matrix bonding. The cement particles appear less integrated, with visible gaps that correlate with higher porosity (~13% at 90 days) and lower bulk density (~2.22 kg/L). On the other hand, for BL-containing sample (*Fig. 8A*), a denser and more compact microstructure is observed, with fewer voids and a more cohesive cement matrix. The enhanced bonding between aggregates and the cement paste supports the lowest porosity (~9% at 90 days) and highest bulk density (~2.28 kg/L), directly contributing to superior mechanical properties.

The SEM image for 2% BL shows the formation of additional C-S-H gels, filling the voids and reducing porosity. This aligns with the observed decrease in apparent porosity from 13% (0% BL) to 9% (2% BL) and the corresponding increase in bulk density from 2.22 kg/L to 2.28 kg/L. The dense microstructure minimizes pathways for crack initiation and water ingress, contributing to improved durability.

The enhanced interfacial bonding visible in the SEM image for 2% BL correlates with the peak compressive strength (~50 MPa at 28 days), splitting tensile strength (~3.6 MPa), and flexural tensile strength (~15 MPa). This demonstrates the role of a compact microstructure in resisting applied stresses. The SEM image for 0% BL highlights a less compact structure with larger voids, which weakens the concrete. This correlates with lower compressive strength (~40 MPa at 28 days) and increased porosity, reducing durability and mechanical performance.

The additional C-S-H gel formation, evidenced in the 2% BL image, results from the pozzolanic reaction of black liquor's organic compounds with calcium hydroxide. This improves matrix densification and reduces porosity [2]. The smoother and more uniform surface of the matrix at 2% BL reflects improved workability and compaction during the mixing process. While not visible in these images, higher BL concentrations (3–4%) are known to disrupt hydration and lead to micro-voids, reducing density and mechanical properties.

The SEM images reinforce the conclusion that 2% BL is the optimal concentration for enhancing both microstructural and macroscopic properties. The denser matrix observed at 2% BL suggests improved resistance to environmental degradation, such as freeze-thaw cycles and chloride ingress.

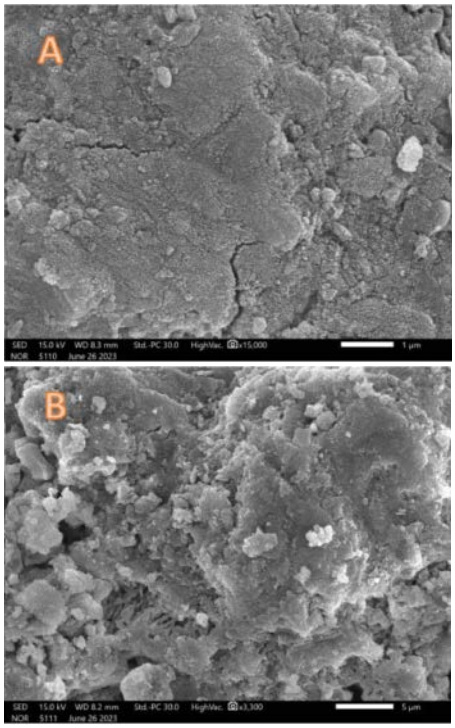


*Fig. 8 SEM images for the BL containing (S2, 2% BL); (A) and pristine (S2); (B) concrete samples*
*8. ábra SEM felvételek a fekete lúg tartalmú (S2, 2% BL); (A) és eredeti (S2); (B) betonmintákról*

## 4. Conclusion

This study demonstrates the potential of black liquor (BL) as an effective and sustainable admixture for concrete. Incorporating BL at an optimal concentration of 2 wt.% significantly enhances the mechanical properties, including compressive strength (66.7% 50 MPa in this study compared to 20~40 MPa in conventional concrete), splitting tensile strength (20% 3.6 MPa in this study compared to 2~4 MPa in conventional concrete), and flexural tensile strength (300% 15 MPa in this study compared to 5 MPa in conventional concrete). Additionally, this concentration results in a denser matrix with reduced porosity (9%) and increased bulk density (2.28 kg/l), as confirmed by microstructural analysis using SEM. The extended setting times observed with BL addition provide improved workability, making it suitable for practical applications. However, excessive BL content (3-4 wt.%) negatively impacts performance due to increased porosity and disrupted hydration dynamics. These findings highlight the dual benefits of performance enhancement and sustainability through the utilization of industrial by-products.

### References

[1] Andrew, R. M. (2018). Global CO 2 emissions from cement production. *Earth System Science Data*, 10(1), 195-217.
[2] METHA, P. (2008). e MONTEIRO, PJM Concrete: Microstructure, properties and materials (in Portuguese). São Paulo: IBRACON.
[3] Siddique, R. (2014). Utilization of industrial by-products in concrete. *Procedia engineering*, 95, 335-347.
[4] Bajpai, P. (2015). *Management of pulp and paper mill waste* (Vol. 431): Springer.
[5] Smook, G. A. (2002). *Handbook for pulp & paper technologists*: A. Wilde.
[6] Neville, A. M. (1995). Properties of concrete. Longman.
[7] Damtoft, J. S., Lukasik, J., Herfort, D., Sorrentino, D., & Gartner, E. M. (2008). Sustainable development and climate change initiatives. *Cement and Concrete Research*, 38(2), 115-127.
[8] Gjørv, O. E. (2009). *Durability design of concrete structures in severe environments*: CRC Press.
[9] Jiang, J., Wang, F., Wang, L., Zhang, J., & Wang, L. (2023). Experimental investigation on effects of polyaniline-modified-lignin on cement-based materials: Strength, hydration and dispersion. *Construction and Building Materials*, 394, 131853.
[10] Chandra, S., & Berntsson, L. (2002). *Lightweight aggregate concrete:* Elsevier.
[11] Celik, K., Jackson, M. D., Mancio, M., Meral, C., Emwas, A.-H., Mehta, P. K., et al. (2014). High-volume natural volcanic pozzolan and limestone powder as partial replacements for portland cement in self-compacting and sustainable concrete. *Cement and Concrete Composites*, 45, 136-147.
[12] Hassan, K., Cabrera, J., & Maliehe, R. (2000). The effect of mineral admixtures on the properties of high-performance concrete. *Cement and Concrete Composites*, 22(4), 267-271.
[13] Neville, A. M., & Brooks, J. J. (1987). *Concrete technology* (Vol. 438): Longman Scientific & Technical England.
[14] Kurtis, K. E. (2015). Innovations in cement-based materials: Addressing sustainability in structural and infrastructure applications. *MRS Bulletin*, 40(12), 1102-1109.
[15] Bajpai, P. (2016). *Pulp and paper industry*: energy conservation: Elsevier.
[16] Chini, S. A., & Mbwambo, W. J. Environmentally friendly solutions for the disposal of concrete wash water from ready mixed concrete operations. In *CIB W89 Beijing International Conference*, 1996 (pp. 21-24): Citeseer
[17] Meyer, C. (2009). The greening of the concrete industry. *Cement and Concrete Composites*, 31(8), 601-605.
[18] Mehta, P. K., & Monteiro, P. (2006). Concrete: microstructure, properties, and materials. (*No Title*).
[19] Abdollahnejad, Z., Hlavacek, P., Miraldo, S., Pacheco-Torgal, F., & Aguiar, J. L. B. d. (2014). Compressive strength, microstructure and hydration products of hybrid alkaline cements. *Materials Research*, 17, 829-837.
[20] Solahuddin, B., & Yahaya, F. A review paper on the effect of waste paper on mechanical properties of concrete. In *IOP Conference Series: Materials Science and Engineering, 2021* (Vol. 1092, pp. 012067, Vol. 1): IOP Publishing
[21] Šeputytė-Jucikė, J., Kligys, M., & Sinica, M. (2016). The effects of modifying additives and chemical admixtures on the properties of porous fresh and hardened cement paste. *Construction and Building Materials, 127*, 679-691.
[22] Mehta, P. (2006). Concrete: Microstructure, Properties, and Materials. McGraw-Hill.
[23] Popovics, S. (1998). *Strength and related properties of concrete: A quantitative approach:* John Wiley & Sons.
[24] Clemens, H., Mayer, S., & Scheu, C. (2017). Microstructure and properties of engineering materials. *Neutrons and synchrotron radiation in engineering materials science: From fundamentals to applications*, 1-20.

Ref.:
**Barakat**, Nasser A. M. – **Nassar**, Mamdouh M. – **Farrag**, Taha E. – **Mohamed**, Hamdy A. A. – **Mahmoud**, Mohamed S.: *Influence of black liquor on concrete performance: a sustainable approachs*
Építőanyag – Journal of Silicate Based and Composite Materials, Vol. 77, No. 1 (2025), 19–27 p.
https://doi.org/10.14382/epitoanyag-jsbcm.2025.4

# GUIDELINE FOR AUTHORS

**The manuscript must contain the followings: title; author's name, workplace, e-mail address; abstract, keywords; main text; acknowledgement** (optional)**; references; figures, photos with notes; tables with notes; short biography** (information on the scientific works of the authors).

**The full manuscript should not be more than 6 pages including figures, photos and tables.** Settings of the word document are: 3 cm margin up and down, 2,5 cm margin left and right. Paper size: A4. Letter size 10 pt, type: Times New Roman. Lines: simple, justified.

**TITLE, AUTHOR**

The title of the article should be short and objective.

**Under the title the name of the author(s), workplace, e-mail address.**

If the text originally was a presentation or poster at a conference, it should be marked.

**ABSTRACT, KEYWORDS**

The abstract is a short summary of the manuscript, about a half page size. The author should give keywords to the text, which are the most important elements of the article.

**MAIN TEXT**

Contains: materials and experimental procedure (or something similar), results and discussion (or something similar), conclusions.

**REFERENCES**

References are marked with numbers, e.g. [6], and a bibliography is made by the reference's order. References should be provided together with the DOI if available.

**Examples:**

Journals:

[6] Mohamed, K. R. – El-Rashidy, Z. M. – Salama, A. A.: In vitro properties of nano-hydroxyapatite/chitosan biocomposites. *Ceramics International.* 37(8), December 2011, pp. 3265–3271, http://doi.org/10.1016/j.ceramint.2011.05.121

Books:

[6] Mehta, P. K. – Monteiro, P. J. M.: Concrete. Microstructure, properties, and materials. *McGraw-Hill*, 2006, 659 p.

**FIGURES, TABLES**

All drawings, diagrams and photos are figures. The **text should contain references to all figures and tables**. This shows the place of the figure in the text. Please send all the figures in attached files, and not as a part of the text. **All figures and tables should have a title**.

**Authors are asked to submit color figures by submission. Black and white figures are suggested to be avoided, however, acceptable.**

The figures should be: tiff, jpg or eps files, 300 dpi at least, photos are 600 dpi at least.

**BIOGRAPHY**

Max. 500 character size professional biography of the author(s).

**CHECKING**

The editing board checks the articles and informs the authors about suggested modifications. Since the author is responsible for the content of the article, the author is not liable to accept them.

**CONTACT**

Please send the manuscript in electronic format to the following e-mail address: femgomze@uni-miskolc.hu and epitoanyag@szte.org.hu or by post: Scientific Society of the Silicate Industry, Budapest, Bécsi út 122–124., H-1034, HUNGARY

**We kindly ask the authors to give their e-mail address and phone number on behalf of the quick conciliation.**




**Építőanyag** – *Journal of Silicate Based and Composite Materials*, Quarterly peer-reviewed periodical of the Hungarian Scientific Society of the Silicate Industry, SZTE.
http://epitoanyag.org.hu